A seven-sex species recognizes self and non-self mating-type via a novel protein complex

Guanxiong Yan[1], Yang Ma[1], Yanfang Wang[2], Jing Zhang[1], Haoming Cheng[1, 3], Fanjie Tan[2], Su Wang[1, 3], Delin Zhang[2], Jie Xiong[1, 4], Ping Yin[2]*, Wei Miao[1, 3, 4, 5]*

[1] Institute of Hydrobiology, Chinese Academy of Sciences, Wuhan 430072, China.
[2] National Key Laboratory of Crop Genetic Improvement, Hubei Hongshan Laboratory, Huazhong Agricultural University, Wuhan 430070, China.
[3] University of Chinese Academy of Sciences, Beijing 100049, China.
[4] Key Laboratory of Breeding Biotechnology and Sustainable Aquaculture, Chinese Academy of Sciences, Wuhan 430000, China.
[5] Hubei Hongshan Laboratory, Wuhan 430000, China.

Corresponding author: Wei Miao, miaowei@ihb.ac.cn.

Ping Yin, yinping@mail.hzau.edu.cn.

Abstract

Although most species have two sexes, multisexual (or multi-mating type) species are also widespread. However, it is unclear how mating-type recognition is achieved at the molecular level in multisexual species. The unicellular ciliate *Tetrahymena thermophila* has seven mating types, which are determined by the MTA and MTB proteins. In this study, we found that both proteins are essential for cells to send or receive complete mating-type information, and transmission of the mating-type signal requires both proteins to be expressed in the same cell. We found that MTA and MTB form a mating-type recognition complex that localizes to the plasma membrane, but not to the cilia. Stimulation experiments showed that the mating-type-specific regions of MTA and MTB mediate both self- and non-self-recognition, indicating that *T. thermophila* uses a dual approach to achieve mating-type recognition. Our results suggest that MTA and MTB form an elaborate multifunctional protein complex that can identify cells of both self and non-self mating types in order to inhibit or activate mating, respectively.

Impact statement

A giant multifunctional protein complex mediates mating-type recognition through a non-ligand-receptor mechanism in a multisexual species.

36 ## Introduction

37 Sexual reproduction is almost universal among eukaryotic organisms. Mating type (or sex) is
38 a key regulatory feature of gamete fusion. Most species have only two sexes/mating types (e.g.,
39 male and female, + and -, or a and α) and species usually use either self- or non-self-recognition
40 mechanism to achieve sex/mating-type recognition (Goodenough & Heitman, 2014). However,
41 species in some lineages, such as some ciliates and basidiomycetes (Heitman, 2015; Phadke &
42 Zufall, 2010), possess multiple mating types, and multiple-alleles self-incompatibility system
43 were observed in some plants, such as Brassicaceae (Iwano & Takayama, 2012; Takayama &
44 Isogai, 2005; Vekemans & Castric, 2021). This raises the interesting question of how
45 sexes/mating types are recognized at the molecular level in multiple sex/mating-type systems.

46 The model unicellular ciliate, *Tetrahymena thermophila*, has seven mating types (I–VII).
47 Under starvation conditions, any cell of one mating type can mate with a cell of any of the other
48 six mating types, but not with one of the same mating type (Figure 1A, Figure 1–figure
49 supplement 1, Video 1–3) (Cervantes et al., 2013; Nanney, 1953; Orias et al., 2017; Yan et al.,
50 2021). Mating-type recognition in *Tetrahymena* depends on direct cell–cell contact (temporary
51 or persistent), which suggests that mating-type proteins localize to the cell surface. However,
52 there is no direct evidence to indicate whether they are ciliary proteins or not. When one cell
53 comes into contact with a cell of a different mating type, a mating-type-dependent recognition
54 event enables both cells to enter a pre-conjugation stage (called costimulation) (Bruns &
55 Palestine, 1975; Finley & Bruns, 1980). Even when cells of different mating types are mixed in
56 unequal ratios (for example, 9 : 1), all cells become fully stimulated (Bruns & Palestine, 1975).

57 This is because one cell can temporarily contact a number of cells and stimulate them. Processes
58 that take place during costimulation include Tip transformation (Wolfe & Grimes, 1979) and
59 concanavalin A (Con-A) receptor appearance (Figure 1B) (Wolfe & Feng, 1988; Wolfe et al.,
60 1986). In preparation for pairing, costimulated cells of the same and different mating type(s)
61 adhere to form very loose pairs. Heterotypic cell pairs form a stable conjugation junction,
62 whereas homotypic pairs separate very quickly (Video 2 and 3) (Kitamura et al., 1986).

63 The mating-type system of *T. thermophila* was described by Nanney and collaborators in the
64 early 1950s (reviewed in (Orias, 1981; Orias et al., 2017)). We previously showed that mating
65 type is determined by a pair of mating-type genes that are organized in head-to-head orientation:
66 *MTA* and *MTB* (Figure 1C) (Cervantes et al., 2013). Each gene has a terminal exon that encodes
67 five transmembrane (TM) helices and a cysteine-rich growth factor receptor (GFR) domain. The
68 region between the two terminal exons of the gene pair encodes the N-terminal mating-type-
69 specific extracellular regions. Based on the mating-type-specific regions, the mating-type genes
70 are called *MTA1-MTB1* for Mating type I, *MTA2-MTB2* for Mating type II and so on. We
71 previously showed that Δ*MTB* cells do not form pairs or produce progeny and that Δ*MTA* cells
72 retain mating-type specificity but pair extremely poorly and rarely produced progeny (Cervantes
73 et al., 2013); we concluded that the two genes are non-redundant and both are essential for
74 mating. In addition, our previous work demonstrated that CDK19, CYC9, and CIP1 are
75 coexpressed with MTA and MTB and are essential for mating. These encoded proteins constitute
76 components of a cyclin-dependent kinase complex, which localizes to the cell tip and pairing
77 junction (Ma et al., 2020). However, challenges such as multiple mating types; the high molecular

78 weight, membrane localization and extremely low expression levels of mating-type proteins; and
79 difficulty in genetically manipulating the mating-type gene locus have so far prevented
80 elucidation of the mode of action of the MTA and MTB proteins and of whether they mediate
81 self- or non-self mating-type recognition.

82 In this study, we provide direct evidence that the MTA and MTB form an elaborate
83 multifunctional protein complex that can identify cells of both self and non-self mating types to
84 inhibit or activate mating, respectively.

85 ## Results

86 **Mating-type recognition cannot be explained by the simple receptor–ligand model**

87 Receptor–ligand interaction is a critical mechanism for intercellular communication that
88 may regulate mating-type recognition in *T. thermophila*, irrespective of whether self- or non-self-
89 recognition mechanisms are employed. Therefore, we first assessed whether mating-type
90 recognition conforms to a straightforward receptor–ligand model (in which one individual
91 mating-type protein acts as the receptor and the other as its ligand) and whether self or non-self
92 is recognized (Figure 2–figure supplement 1A, 1 and 2). For this, we determined whether
93 deletion of each mating-type gene affected the transmission and detection of mating signals to
94 and from wild-type (WT) cells (Figure 2A shows the experimental procedure) by assessing the
95 ability of cells to undergo costimulation (the prerequisite for mating). Our experiment allows us
96 to test if cells missing one of the two mating-type proteins can still costimulate WT cells (detailed
97 explain refers to Figure 2–figure supplement 1A, 3–6).

98 In *T. thermophila*, cells normally enter into the fully costimulation stage within ~30 min after
99 mixing starved WT cells of two different mating types, and start pair formation during the next
100 ~30 min (Figure 2B, black line). Cells that have already been costimulated immediately start
101 forming pairs with other costimulated cells of a different mating type (Figure 2B, red line).

102 To our surprise, the rate of pair formation in WT cells pre-incubated with either Δ*MTA* cells
103 (Figure 2B, green line) or Δ*MTB* cells (Figure 2B, blue line) did not increase (i.e., costimulation did
104 not occur). It indicated that neither the MTA protein from Δ*MTB* cells nor the MTB protein from
105 Δ*MTA* cells can stimulate the WT cell, which does not fit any deductions based on the simple
106 receptor–ligand model we proposed (Figure 2–figure supplement 1A). These results were not
107 changed by extending the pre-incubation time (Figure 2–figure supplement 1C). Therefore, both
108 MTA and MTB proteins are essential for the mating-type signal; there is no simple receptor–
109 ligand relationship.

110 In addition, WT cells were not costimulated even when they were simultaneously incubated
111 with both Δ*MTA* and Δ*MTB* cells (Figure 2B, teal line), although, according to the receptor–ligand
112 model, they should have received "MTA stimulation" from Δ*MTB* cells and "MTB stimulation"
113 from Δ*MTA* cells. This result indicates that the absence of a mating-type protein in one cell
114 cannot be complemented by its presence in another cell in the same culture; the MTA and MTB
115 proteins must be in the same cell to transmit the mating-type signal. This finding also suggests
116 that mating-type recognition cannot be explained by a simple receptor–ligand model. It is
117 possible that the MTA and MTB proteins form a complex which either serves as a recognizer
118 (functioning as both ligand and receptor) or a co-receptor. But, since MTA and MTB are the only

119 genes with mating-type-specificity, it is unlikely that the complex is acting as a co-receptor.
120 Whether MTA and MTB act as a ligand and a receptor independently within the complex will be
121 discussed later.

122 **Mating-type proteins differentially regulate two steps of costimulation**

123 During costimulation, cells undergo a sequence of developmental events that remodel the
124 anterior cell membrane and its associated cytoskeleton (Cole, 2013). Two hallmarks of this
125 process are Tip transformation (in which the anterior tip of the cell becomes curved) and Con-A
126 receptor appearance (receptors bound by the plant lectin concanavalin A, which binds to
127 mannose containing glycoproteins). When WT cells of one mating type were mixed with WT cells
128 of another mating type, the cell tips became transformed (Figure 2C, 4) and Con-A receptors
129 appeared in almost all cells (Figure 2D, 4). When WT cells were pre-incubated with Δ*MTA*, Δ*MTB*,
130 or both cell types, Tip transformation was not observed in any cell (Figure 2C, 5–7). Similarly,
131 when cells of each mutant were pre-incubated with WT cells, Tip transformation was not
132 detected (Figure 2C, 8 and 9). The outcome was slightly different for Con-A receptor appearance.
133 Con-A receptors were not observed in WT cells pre-incubated with Δ*MTB* cells (Figure 2D, 6) or in
134 cells of either mutant pre-incubated with WT cells (Figure 2D, 7 and 8). In contrast, when WT
135 cells were exposed to Δ*MTA* or "Δ*MTA* cells plus Δ*MTB* cells", the Con-A receptor was detected
136 (Figure 2D, 5 and 9); this is consistent with Δ*MTA* cells retaining a very weak ability to pair
137 (Cervantes et al., 2013). These results indicate that neither Δ*MTA* and Δ*MTB* cells can fully
138 stimulate WT cells or be stimulated by WT cells. They also demonstrate that costimulation can be

139 separated into two stages: (i) one represented by the appearance of Con-A receptors that only
140 requires MTB protein in partner cells, and (ii) the other represented by morphological
141 transformation of the cell tip, which requires both MTA and MTB.

142 **Mating-type proteins form a complex with several coexpressed proteins**

143 According to the pre-incubation results with "Δ*MTA* cells plus Δ*MTB* cells", MTA and MTB
144 cannot functionally complement each other when expressed on different cells (Figure 2B, teal;
145 Figure 2C, 7). In contrast, we previously found that Δ*CDK19* and Δ*CYC9* cells, which express both
146 MTA and MTB, cannot mate. Pre-incubation WT cells with each of them of different mating types
147 promotes WT cells mating. (Ma et al., 2020). The difference in results between these two types
148 of pre-incubation may be caused by whether MTA and MTB proteins are expressed on the same
149 or different cells: Since TM helices fix the proteins onto the cytomembrane, the mating-type
150 proteins are limited on each cell. Thus, in Δ*MTA* and Δ*MTB* cells, the remaining mating-type
151 protein expressed on different cells (MTB or MTA individually) is likely to be spatially separated.
152 WT cells, even when pre-incubated with both Δ*MTA* and Δ*MTB* cells simultaneously, receive MTB
153 or MTA signals separately (Figure 2–figure supplement 1G). However, in Δ*CDK19* and Δ*CYC9* cells,
154 MTA and MTB proteins are expressed on the same cell, allowing them to provide MTA and MTB
155 signals together (Figure 2–figure supplement 1E). These findings lead us to propose the
156 hypothesis that MTA and MTB proteins form a mating-type recognition complex (MTRC).

157 To test whether MTA and MTB proteins physically interact, an HA-tag coding sequence was
158 ligated to the 3' end of the *MTA* gene (Figure 3A); cellular proteins were co-precipitated with HA-

159 tagged MTA and analyzed by immunoprecipitation-coupled mass spectrometry (IP-MS). As
160 expected, the MTB protein co-purified with MTA (Figure 3B, C), as did another set of proteins,
161 which we named MRC1–MRC6 (Figure 3B, C and Figure 3–Source data 1 and 2). Next, we
162 produced strains expressing either HA-tagged MTB or MRC1 (Figure 3A), and found that each
163 protein pulled down a subset of the proteins that co-purified with MTA (Figure 3B, C).
164 Unfortunately, these pull-down experiments were not as successful as the MTA IPs, perhaps
165 because of the higher molecular weight of MTB (194 kDa) and MRC1 (212 kDa). Taken together,
166 our results suggest that MTA, MTB, and MRC1–MRC6 form the MTRC. Alternatively, MTA and
167 MTB may interact with subsets of MRC proteins to form smaller complexes or alternative MTRCs.
168 Different protein interactors were identified in extracts from cells at different mating stages. This
169 may reflect conformational changes in the MTRC but the huge molecular weight of the complex
170 and extremely low expression levels of its proteins make this possibility difficult to investigate.

171 All the identified components of MTRC are large membrane proteins (predicted size, 92–
172 212 kDa). Figure 3D shows the predicted domains of the MRC1–MRC6 proteins. Like MTA and
173 MTB, MRC1 has five predicted TM helices and a GFR domain. MRC2 has eight TM helices and a
174 pectin lyase-fold domain, suggesting a possible role in carbohydrate chain modification. MRC3
175 has two TM helices in the central region and an adjacent ~35 amino acid (aa) poly-E region.
176 MRC4 and MRC5 (previously named TPA9 (Wang et al., 1997; Wang & Takeyasu, 1997)) are both
177 P-type ATPases that are likely to function as calcium-translocators. MRC6 has four TM helices and
178 a P-loop containing nucleoside triphosphate hydrolases. Most of the MRC genes are highly
179 coexpressed with *MTA* and *MTB* (Figure 3E). Examination of the whole genome sequences of

180 strains with mating types II–VII, confirmed that only the sequences of *MTA* and *MTB* genes are
181 mating-type-specific.

182 In addition to the MRC proteins, CDK19, CYC9, CIP1, and AKM3 were identified in IP-MS
183 experiments, but with relatively few supporting peptides (Figure 3C). CDK19, CYC9, and CIP1
184 have been proved to be essential for mating (Ma et al., 2020). AKM3 is predicted to be a K^+
185 channel of unknown biological function. It is coexpressed with *MTA* and *MTB* (Figure 3E), and we
186 found that the *AKM3* deletion strain cannot pair. Therefore, these four proteins are also likely to
187 interact with the mating-type proteins (perhaps indirectly and/or via weak interactions) and
188 might be involved in downstream signaling following mating-type recognition.

189 **Mating-type proteins localize to the cell surface but not to the cilia**

190 We used the MTA7-HA strain to determine the localization of mating-type proteins. Cell
191 fractionation (Figure 4–figure supplement 1) revealed that MTA7-HA is a membrane protein
192 (Figure 4A). Biotinylation and isolation of cell surface proteins confirmed that MTA7-HA is
193 exposed on the cell surface (Figure 4B). To investigate whether MTA7-HA localizes to the cilia
194 membrane, we isolated and collected cilia (Figure 4C) and then analyzed cilia protein extracts by
195 IP-coupled western blotting (WB) and MS. MS analysis identified typical ciliary proteins, such as
196 inner and outer arm dynein proteins (Figure 4–Source data 1). However, both IP-WB (Figure 4D)
197 and MS (Figure 4–Source data 1) consistently failed to identify MTA7-HA protein in the cilia
198 fraction. These results conclusively indicate that MTA7-HA localizes to the cell surface, but not to
199 cilia. Unfortunately, we failed to detect MTA7-HA by immunofluorescence staining of cells at any

200 mating stage (starvation, costimulation, or conjugation), probably due to the epitope masking
201 and extremely low expression level.

202 To further examine localization of the mating-type proteins, eGFP-tagged MTB2 was
203 overexpressed from an exogenous locus (Figure 4E). This strain (which has a mating type VI
204 background) mated normally with WT cells of all mating types except for VI and II. This result
205 indicates the overexpressed MTB2-eGFP protein is fully functional for mating. Interestingly, cells
206 of this strain can also mate with one another (self-mating); a similar phenotype was previously
207 reported for strains expressing multiple mating-type proteins (Lin & Yao, 2020). These selfing
208 ability may be caused by the interaction between heterotypic MTRCs. The overexpressed MTB2-
209 eGFP protein was detected on the cell surface in a linear pattern radiating from the cell tip to the
210 cell body along the ciliary rows (Figure 4F, costimulated cell; Figure 4G, mating pair), although
211 signals are also apparent between ciliary rows. Co-staining with a tubulin dye showed that the
212 MTB2-eGFP protein is adjacent to, rather than co-localizing with, the base of cilia (Figure 4F, G,
213 enlarged). Confocal images from the interior of the cell and through the cilia showed that MTB2-
214 eGFP localizes to the cell surface (and also to intracellular structures, probably the endoplasmic
215 reticulum (ER) and Golgi), but not to the cilia (Figure 4–figure supplement 2), confirming our
216 results with the MTA7-HA protein (Figure 4A-D). MS analysis showed that overexpressed MTB2-
217 eGFP protein was not present in isolated cilia of the *MTB2-eGFP* strain (Figure 4–Source data 2).
218 Therefore, mating-type proteins localize to the cell surface, as might be expected since mating-
219 type recognition depends on cell–cell contact.

220 **Mating-type proteins influence non-self-recognition**

221 The mating-type-specific region of the *MTA* and *MTB* gene pair is the only known genetic
222 locus with mating-type specificity; therefore, we next tested whether this region influences self-
223 and/or non-self mating-type recognition. For this, we expressed the extracellular region of MTA
224 (MTAxc) or MTB (MTBxc) in an insect cell secreted expression system, purified the recombinant
225 proteins (Figure 5–figure supplement 1), and then tested their effect on mating behavior.

226 First, we tested whether MTAxc and MTBxc can influence mating in cells with a different
227 mating-type specificity (i.e., non-self-recognition). When WT cells were incubated with MTAxc
228 (and/or MTBxc) of a different mating type, markers of costimulation were not observed (Figure
229 5–figure supplement 2). Surprisingly, treated cells had a significantly increased pairing rate.
230 Compared with controls (Figure 5A–C, black), WT cells (VI and VII) pre-treated with MTAxc or
231 MTBxc of different mating types (VII and VI, respectively) had a similar increased pairing rate
232 (Figure 5A–C, green or blue). It with a stronger effect (synergistic effect) after pre-treatment with
233 both MTAxc and MTBxc (Figure 5A–C, teal), consistent with our finding that MTA and MTB
234 interact with each other (Figure 2–figure supplement 1F). Dose–effect assays showed that
235 pairing rates increased with increasing MTA6xc and MTB6xc concentrations between 3 pg/ml
236 and 30 pg/ml, with the effect becoming saturated or weaker at higher concentrations
237 (Figure 6A–F). MTAxc and MTBxc also stimulated mating for all other WT mating types (Figure 6G,
238 H), indicating that this is a general effect. Based on these results, we conclude that the mating-
239 type-specific regions of MTA and MTB proteins are involved in non-self mating-type recognition.

240 This results also shed on whether MTA and MTB act independently as a ligand and a
241 receptor within the complex. For instance, if MTA is a ligand and MTB is a receptor, treating a cell
242 with MTAxc protein should induce a mating signal, whereas treatment with MTBxc should not.
243 However, our results indicate that MTAxc and MTBxc have very similar effects, and the effect is
244 stronger when treated with two proteins together. Therefore, this possibility is unlikely. In
245 addition, we did not identify any costimulation markers when incubated with MTAxc and/or
246 MTBxc. This may be due to the lack of other components, differences in post-translational
247 modifications between insect cells and *Tetrahymena*, or variations in protein conditions between
248 the cell membrane and solution.

249 **Mating-type proteins also influence self-recognition**

250 We used similar methods to examine whether pre-treatment with a cognate mating-type-
251 specific region (i.e., self-recognition) affects mating. Treatment of WT cells (VI and VII) with
252 MTAxc and/or MTBxc of the same mating type decreased the pairing rate (Figure 5D, E, green or
253 blue). No obvious difference was found between treatments with MTAxc and MTBxc. Meanwhile,
254 a significant synergistic effect was observed (Figure 5D, E, teal). For all treatments (single or
255 combined), the pairing rate was similar by 4 h (reaching >80%; Figure 5D, F), indicating that the
256 initial inhibitory effect on pairing was eventually overcome. Negative regulation by MTAxc and
257 MTBxc was also observed for other mating-type combinations (Figure 6I, J). These results
258 support the idea that the mating-type-specific regions of MTA and MTB proteins mediate both
259 non-self (between different mating types) and self (between the same mating type) recognition.

260 **Discussion**

261 Although the basic biological features of the *T. thermophila* mating-type system were
262 discovered over half a century ago, the mechanism for mating-type recognition remains unclear.
263 Here, we identified a novel MTRC that contains MTA, MTB, and several other proteins and
264 provide evidence that MTA and MTB mediate both self and non-self mating-type recognition.

265 An open question is why *T. thermophila* should use such a dual approach (both self and non-
266 self) to achieve mating-type recognition. Recent research on basidiomycetes and flowering
267 plants (other species with multiple mating types) has shown that their mating-type recognition
268 (or self-incompatibility) mechanisms involve either self- or non-self-recognition (Fraser &
269 Heitman, 2003; Iwano & Takayama, 2012; Vekemans & Castric, 2021). Our previous evolutionary
270 study showed that the length of the mating-type-specific region differs significantly among
271 different *Tetrahymena* species (~2000 aa for *T. thermophila*, ~3200 aa for *T. borealis*, while only
272 ~1000 aa for *T. pigmentosa*) (Yan et al., 2021). Based on the massive difference in length, it is
273 reasonable to speculate that different species might use different mechanisms for mating-type
274 recognition. Therefore, dramatic evolution of the mating-type recognition mechanism seems to
275 have occurred relatively soon after the emergence of the *Tetrahymena* genus. Further detailed
276 functional and evolutionary studies may reveal whether the mating-type recognition model
277 differed in different *Tetrahymena* species, and how and why this recognition mechanism evolved
278 and how its evolution contributed to speciation.

279 MTRC is likely to be a giant protein complex which is over a million Daltons in size. The large
280 protein complex formed is reminiscent of the fusion patches that develop in budding or fission

281 yeasts. In these species, the mating type receptors are activated by ligand pheromones from the
282 opposite mating type that induce polarity patch formation (see (Sieber et al., 2023) for a recent
283 review). At these patches, growth (shmooing) and fusion occur, which is reminiscent (in a
284 different order) of the tip transformation in *T. thermophila*. Future studies of this protein
285 complex may reveal whether more similar processes and/or mechanisms shared in these two
286 distant lineages.

287 We still do not know what intracellular signals are transduced when the MTRCs on two cells
288 interact. Mating-type self-recognition might generate an inhibitory signal or might simply
289 inactivate the MTRC. In many species, such as *Papaver rhoeas* and *Ciona intestinalis*, interaction
290 between mating-type proteins of the same mating type induces changes in cytoplasmic Ca^{2+}
291 concentration that cause self-incompatibility (Giamarchi et al., 2006; Harada et al., 2008; Wu et
292 al., 2011). A similar system may exist in *T. thermophila*, since the MRC4 and MRC5 proteins are
293 predicted to be Ca^{2+}-translocators. Interaction between MTRCs on cells of different mating types
294 (non-self-recognition) should result in their activation to allow the cells to initiate pairing. We
295 propose that the activation signal involves the CDK19 complex (a cyclin-dependent kinase
296 complex) (Ma et al., 2020) and AKM3 (a K^+ channel; Figure 3C) because they probably interact
297 with the MTRC. We expect future studies to lead to the discovery of more detailed mechanisms
298 for mating-type recognition and initiation of conjugation involving these proteins. An intriguing
299 discovery is that the *MTB2-eGFP* cell (VI background) can undergo selfing and mate with cells of
300 all other mating types except VI and II. The inability to mate with VI and II supports the self-
301 recognition model. Additionally, in theory, there should be two types of MTRCs in the *MTB2-*

302 *eGFP* cell: MTRC of pure VI specificity (A6B6) and heterotypic MTRC of MTA6 and MTB2 (A6B2).
303 Consequently, opposite mating-type recognition outcomes should occur simultaneously when
304 the *MTB2-eGFP* cell recognizes another *MTB2-eGFP* cell: inhibition (A6B6-A6B6) and activation
305 (A6B2-A6B2). The overall observed result showed that this strain can self, indicating there is no
306 (MTRC is only blocked) or relatively weak inhibitory signal generated during self-recognition.

307 *Paramecium tetraurelia*, a closely related Oligohymenophorean ciliate, has only two mating
308 types, which are determined by the expression or non-expression of a *Tetrahymena*-MTA/B-like
309 protein called mtA (Singh et al., 2014; Yan et al., 2021). An intriguing question is whether mtA
310 also engages in the formation of a MTRC with other proteins by serving as a recognizer rather
311 than mediating a straightforward receptor–ligand interaction. Future investigations of
312 *Paramecium tetraurelia* may shed light on the origins and evolutionary aspects of this distinctive
313 mating system. Moreover, due to the extremely long evolutionary distance, recognition
314 mechanisms discovered in model species fall short of explaining many of the intricate biological
315 events in protists. Insight into the detailed function of MTRC could contribute to our
316 understanding of cell–cell recognition processes in other species, such as *Toxoplasma* and
317 *Plasmodium*.

318 Materials and Methods

319 Biological methods

320 Strains used in this study are summarized in Appendix 1–table 1. All cell growth, starvation, and
321 pairing experiments were conducted at 30°C. Cells were grown in Super Proteose Peptone (SPP)
322 medium (1% Proteose Peptone, 0.1% yeast extract, 0.2% glucose, 0.003% Sequestrene) or Neff

323 medium (0.25% Proteose Peptone, 0.25% yeast extract, 0.5% glucose, 0.003% Sequestrene). Cells
324 were starved in 10 mM Tris-Cl (pH 7.4) for ~16 h before all pairing experiments. For normal
325 pairing assays, equal numbers of starved cells of different mating types (at ~2×10^6 cells/ml) were
326 mixed. To obtain costimulated (pre-incubated) cells, two starved strains were mixed at a 9 : 1
327 ratio for ~30 min (unless otherwise stated). Before mixing costimulated cells, any potentially
328 pairing cells were separated by shaking. Figure 2A shows the setup of costimulation experiments.
329 For all mating experiments (whether or not they involved mutant cells), the starting WT cell
330 density was ~2×10^6 cells/ml. To prepare starvation medium containing mating-essential factors,
331 *Tetrahymena* cells (~2×10^6 cells/ml) were starved in fresh medium for ~16 hours. Subsequently,
332 cells were removed through three rounds of centrifugation (1000 g, 3 min each). The following
333 formula was used to calculate pairing ratios and correct for the presence of mutant cells:

334 $$\%cells\ paired = \frac{2 \times \#\ pairs}{(2 \times \#\ pairs + \#\ unpaired\ cells) \times \%\ WT\ cells} \times 100$$

335 **Somatic gene deletion, truncation, and protein tagging**

336 To construct deletion strains, a ~1 kb fragment upstream of the gene's open reading frame (ORF)
337 (#1), a ~0.5 kb fragment downstream of the gene's ORF (#2), and a ~1 kb fragment downstream
338 of #2 (#3) were amplified. Fragments #2 and #3 were joined to the *NEO4* cassette (Cd^{2+}-inducible
339 *MTT1* promoter linked to the neomycin resistance gene) by fusion PCR and then cloned into the
340 pBlueScript SK (+) vector together with fragment #1. In this way, #1-#2-*NEO4*-#3 constructs were
341 obtained for the next transformation. HA-tagged strains were constructed in a similar way,
342 except that fragment #1 was upstream of the stop codon or upstream of the terminal intron. To
343 obtain the MTB2-eGFP construct, MTB2-coding sequences replaced the MTT1-coding sequence

344 (Figure 4E) and the construct was made using the large DNA fragment assembly method (Jiang et
345 al., 2022). Constructs were introduced into starved WT cells by biolistic transformation to obtain
346 deletion strains (Mochizuki, 2008). Positive clones were selected in SPP medium containing
347 decreasing Cd^{2+} concentrations (from 1 μg/ml to 0.05 μg/ml) and increasing paromomycin
348 concentrations (from 120 μg/ml to 40 mg/ml) until all WT somatic chromosomes had been
349 replaced by mutant ones, as determined by PCR using checking primers. All primers used are
350 listed in Appendix 1–table 2.

351 **Immunoprecipitation and mass spectrometry**

352 The IP method was adapted from a published method (Tian et al., 2017). To pull down HA-tagged
353 proteins from *T. thermophila*, cells were harvested from 500 ml cultures (density ~3×10^6 cells/ml).
354 Cells were then treated for 20 min with paraformaldehyde (PFA) (at a final concentration of 0.3%)
355 to stabilize protein–protein interactions, washed with PB buffer (2.7 mM KCl, 8 mM Na_2HPO_4,
356 1.5 mM K_2HPO_4), and blocked with 125 mM glycine. Cells were then resuspended in lysis buffer
357 (1% Triton X-100, 30 mM Tris-HCl, 20 mM KCl, 2 mM $MgCl_2$, 1 mM phenylmethylsulfonyl fluoride,
358 150 mM NaCl, cOmplete proteinase inhibitor [Roche Diagnostics, Indianapolis, IN, USA]), lysed by
359 ultrasonic treatment and incubated with EZview anti-HA agarose beads (Sigma-Aldrich, St Louis,
360 MO, USA) for 2.5 h at 4°C. The beads were washed with wash buffer (1% Triton X-100, 600 mM
361 NaCl, 30 mM Tris-HCl, 20 mM KCl, 2 mM $MgCl_2$, cOmplete proteinase inhibitor) to remove
362 nonspecific-binding proteins and then HA-tagged proteins were eluted with HA peptides (Sigma-
363 Aldrich). WT samples (not HA tagged) were run in parallel for each sample. In total, data for 13
364 WT controls were combined to identify non-specific binding proteins.

365 For MS, the EASY-nLC chromatography system (Thermo Scientific, Rockford, IL, USA) was
366 coupled on-line to an Orbitrap Elite instrument (Thermo Scientific) via a Nanospray Flex Ion
367 Source (Thermo Scientific). Xtract software (Thermo Scientific) and Proteome Discoverer 2.1
368 software were used for MS data analysis based on a database that combines the 2014 version of
369 whole genome protein annotation (http://ciliate.org/index.php/home/downloads, which
370 contains the whole length sequence of MTA6 and MTB6) and mating-type-specific regions of all
371 other mating-type proteins. IP data were analyzed using CRAPome (Mellacheruvu et al., 2013).

372 **Membrane protein extraction**

373 Figure 4–figure supplement 1A shows the workflow used for membrane protein extraction. Cells
374 were collected, resuspended in 20 ml lysis buffer (150 mM NaCl, 25 mM HEPES, 10% glycerol,
375 2 mM PMSF, 2.6 µg/ml aprotinin, 1.4 µg/ml pepstatin, 10 µg/ml leupeptin, pH 7.4), and lysed by
376 high-pressure homogenization. The lysate was clarified first at low speed (14,000 rpm, 4°C,
377 15 min), and then at high speed (150,000 g, 4°C, 1 h). The pellet was resuspended in 5 ml lysis
378 buffer containing 1% DDM (Anatrace, Maumee, OH, USA) and rotated for 2 h at 4°C to extract
379 the membrane proteins. Undissolved material was removed by centrifugation (14,000 rpm, 4°C,
380 30 min). The membrane protein extract was incubated with EZview anti-HA agarose beads for
381 2.5 h at 4°C and then washed with 5 ml lysis buffer.

382 **Biotinylation and isolation of cell surface proteins**

383 Pierce Cell Surface Protein Biotinylation and Isolation Kit (Thermo Scientific) was used to
384 biotinylate and isolate cell surface proteins. For this, 75 ml cells (density ~3×10^6 cells/ml) were
385 harvested and washed once with BupH phosphate-buffered saline (PBS; 137 mM NaCl, 2.7 mM

386 KCl, 4.3 mM Na_2HPO_4, 1.4 mM KH_2PO_4). Cells were then resuspended in 75 ml PBS containing
387 0.72 mg/ml Sulfo-NHS-SS-biotin and incubated at room temperature for 10 min. After two
388 washes with 50 ml ice-cold BupH Tris buffer, cells were resuspended in 3 ml lysis buffer (PBS
389 containing 1% Triton X-100, 1 mM phenylmethylsulfonyl fluoride and cOmplete proteinase
390 inhibitor [Roche Diagnostics]), lysed by ultrasonic treatment and incubated with 1.2 ml
391 NeutrAvidin Agarose for 0.5 h at room temperature. The resin was washed four times with 0.5 ml
392 wash buffer and then cell surface proteins were eluted with 1.2 ml elution buffer (with 10 mM
393 DTT). Before WB, cell surface protein samples were concentrated into 0.1 ml volumes using a
394 30 kDa centrifugal concentrator (Merck Millipore).

395 **Ciliary protein collection**

396 To remove cilia, 500 ml cells (density ~3×10^6 cells/ml) were harvested at room temperature and
397 resuspended in 25 ml 10 mM Tris-Cl (pH 7.4), to which 50 ml medium A (10 mM $EDTA_2Na$,
398 50 mM sodium acetate, pH 6.0) was added. After 30 s, 25 ml cold distilled water was added;
399 1 min later, 0.25 ml 0.4 M $CaCl_2$ was added and incubated for 15 s. The cilia were detached from
400 the calcium-shocked cells by vortexing three times for 5 s at 15 s intervals. To collect the cilia, cell
401 bodies were removed by two rounds of centrifugation at 1500 rpm for 5 min at 4°C, and then
402 cilia were collected by centrifugation at 15000 rpm for 15 min at 4°C.

403 **Cytological methods**

404 Fluorescein-labeled Con-A labeling was performed as previously reported (Ma et al., 2020). In
405 brief, cells were fixed and stained with fluorescein-labeled Con-A (Vector Laboratories,
406 Burlingame, CA, USA) at 37.5 μg/ml for 5 min and then washed three times with PB buffer.

407 For analysis of Tip transformation, cells were observed and photographed as soon as possible
408 after fixation with 1% PFA. To distinguish between cell strains in a pairing mixture, starved cells
409 of one strain were labeled with 500 nM MitoTracker (Invitrogen, Eugene, OR, USA), followed by
410 two washes with 10 mM Tris-Cl (pH 7.4) before mixing.
411 For tubulin staining, cells were collected and fixed in PHEM buffer (30 mM PIPES, 14 mM HEPES,
412 5 mM EGTA and 2 mM $MgSO_4$) containing 1% PFA and incubated for 30 min at 4°C. After three
413 washes with PBS (10 min each), Tubulin-Atto 594 was added and incubated for 1 h at 25°C. Finally,
414 cells were washed three times with PBS (10 min each).
415 **Expression and purification of the extracellular region of mating-type proteins**
416 Coding sequences of the extracellular region of mating-type proteins (MTA6xc, MTB6xc, MTA7xc,
417 and MTB7xc) were codon-optimized and synthesized for expression in an insect-cell system
418 (*Trichoplusia ni* Hi5 cells). Codon-optimized sequences were cloned into pFastBac vectors
419 containing an N-terminal hemolin signal peptide sequence and a C-terminal 10×His tag sequence.
420 The obtained constructs were transformed into competent DH10Bac cells and individual bacmids
421 were transfected into *Spodoptera frugiperda* Sf9 cells. Recombinant Baculoviruses were
422 collected after 4 days and used to infect *Trichoplusia ni* Hi5 cells for protein expression. Proteins
423 were harvested 60 h after infection and purified with Ni-NTA Superflow resin (Qiagen), anion-
424 exchange chromatography (Source 15Q, GE Healthcare), and size-exclusion chromatography
425 (Superdex-200 Increase 10/300, GE Healthcare).

426 **Bioinformatics analysis**

427 All microarray data were derived from *Tetra*FGD (Xiong et al., 2011) (http://tfgd.ihb.ac.cn/). DNA
428 sequencing data for mating type II–VII cells are derived from a previous report (Wang et al.,
429 2020). Compute pI/Mw (https://web.expasy.org/compute_pi/) was used to predict protein
430 molecular weight. InterProScan (http://www.ebi.ac.uk/interpro/) was used for function and
431 domain annotation (Jones et al., 2014).

432 **Statistical analysis**

433 For mating experiments, more than 100 unpaired cells or cell pairs were counted, with three to
434 five independent replicates. GraphPad software (version 8.0.2) was used for statistical analysis
435 based on ANOVA (matched, Fisher's LSD test).

436 **Acknowledgments**

437 We thank Eduardo Orias (University of California Santa Barbara), Eileen P. Hamilton (University of
438 California Santa Barbara), and Kazufumi Mochizuki (University of Montpellier) for their help and
439 suggestions about experiment design and manuscript writing, and Yunfei Wei (Huazhong
440 University of Science and Technology) for tubulin staining using Tubulin-Atto 594. We also thank
441 members of the Protist 10,000 Genomes Project (P10K) consortium for helpful suggestions. We
442 would like to thank Min Wang at the Analysis and Testing Center of Institute of Hydrobiology,
443 Chinese Academy of Sciences for her help with mass spectrometry. The bioinformatics analysis
444 was supported by the Wuhan Branch, Supercomputing Center, Chinese Academy of Sciences,
445 China. Culture and maintenance of *Tetrahymena* cells were supported by the National Aquatic
446 Biological Resource Center (NABRC).

Funding information

This work was funded by National Natural Science Foundation of China (No. 32130011), Bureau of Frontier Sciences and Education, Chinese Academy of Sciences (No. ZDBS-LY-SM026), National Natural Science Foundation of China (No. 32200344) and China Postdoctoral Science Foundation (No. 2021M703433).

Author Contributions

G.Y. performed the experiments and analyzed the data. Y.M and H.C helped to construct mutants and perform cellular experiments. Y.W. and F.T. performed protein expression and purification experiments. J.Z helped to maintenance of *Tetrahymena* strains. G.Y. wrote the manuscript. All of the authors helped to conceptualize the work, and edit the text and the figures. W.M. and P.Y. supervised the work.

Conflict of Interest

Authors declare that they have no competing interests.

References

Adair, W. S., Barker, R., Turner, R. S., & Wolfe, J. (1978). Demonstration of a cell-free factor involved in cell interactions during mating in *Tetrahymena*. *Nature*, *274*(5666), 54-55.

Bruns, P. J., & Palestine, R. F. (1975). Costimulation in *Tetrahymena pyriformis*: A developmental interaction between specially prepared cells. *Developmental Biology*, *42*(1), 75-83. https://doi.org/https://doi.org/10.1016/0012-1606(75)90315-2

Cervantes, M. D., Hamilton, E. P., Xiong, J., Lawson, M. J., Yuan, D., Hadjithomas, M., Miao, W., & Orias, E. (2013). Selecting one of several mating types through gene segment joining and deletion in *Tetrahymena thermophila*. *PLOS Biology*, *11*(3), e1001518. https://doi.org/10.1371/journal.pbio.1001518

Cole, E. S. (2013). *The Tetrahymena Conjugation Junction. In: Madame Curie Bioscience Database [Internet].* Landes Bioscience.

472 Finley, M. J., & Bruns, P. J. (1980). Costimulation in *Tetrahymena* II. A nonspecific response to
473 heterotypic cell-cell interactions. *Developmental Biology*, *79*(1), 81-94.
474 https://doi.org/https://doi.org/10.1016/0012-1606(80)90074-3
475 Fraser, J. A., & Heitman, J. (2003). Fungal mating-type loci. *Current Biology*, *13*(20), R792-795.
476 https://doi.org/10.1016/j.cub.2003.09.046
477 Fujishima, M., Tsuda, M., Mikami, Y., & Shinoda, K. (1993). Costimulation-induced rounding in
478 *Tetrahymena thermophila*: early cell shape transformation induced by sexual cell-to-cell
479 collisions between complementary mating types. *Developmental Biology*, *155*(1), 198-205.
480 https://doi.org/10.1006/dbio.1993.1018
481 Giamarchi, A., Padilla, F., Coste, B., Raoux, M., Crest, M., Honore, E., & Delmas, P. (2006). The versatile
482 nature of the calcium-permeable cation channel TRPP2. *EMBO Reports*, *7*(8), 787-793.
483 https://doi.org/10.1038/sj.embor.7400745
484 Goodenough, U., & Heitman, J. (2014). Origins of eukaryotic sexual reproduction. *Cold Spring Harbor*
485 *Perspectives in Biology*, *6*(3). https://doi.org/10.1101/cshperspect.a016154
486 Harada, Y., Takagaki, Y., Sunagawa, M., Saito, T., Yamada, L., Taniguchi, H., Shoguchi, E., & Sawada, H.
487 (2008). Mechanism of self-sterility in a hermaphroditic chordate. *Science*, *320*(5875), 548-
488 550.
489 Heitman, J. (2015). Evolution of sexual reproduction: a view from the Fungal Kingdom supports an
490 evolutionary epoch with sex before sexes. *Fungal Biology Reviews*, *29*(3-4), 108-117.
491 https://doi.org/10.1016/j.fbr.2015.08.002
492 Iwano, M., & Takayama, S. (2012). Self/non-self discrimination in angiosperm self-incompatibility.
493 *Current Opinion in Plant Biology*, *15*(1), 78-83. https://doi.org/10.1016/j.pbi.2011.09.003
494 Jiang, S., Tang, Y., Xiang, L., Zhu, X., Cai, Z., Li, L., Chen, Y., Chen, P., Feng, Y., Lin, X., Li, G., Sharif, J., &
495 Dai, J. (2022). Efficient de novo assembly and modification of large DNA fragments. *Sci China*
496 *Life Sci*, *65*(7), 1445-1455. https://doi.org/10.1007/s11427-021-2029-0
497 Jones, P., Binns, D., Chang, H. Y., Fraser, M., Li, W., McAnulla, C., McWilliam, H., Maslen, J., Mitchell,
498 A., Nuka, G., Pesseat, S., Quinn, A. F., Sangrador-Vegas, A., Scheremetjew, M., Yong, S. Y.,
499 Lopez, R., & Hunter, S. (2014). InterProScan 5: genome-scale protein function classification.
500 *Bioinformatics*, *30*(9), 1236-1240. https://doi.org/10.1093/bioinformatics/btu031
501 Kitamura, A., Sugai, T., & Kitamura, Y. (1986). Homotypic pair formation during conjugation in
502 *Tetrahymena thermophila*. *Journal of Cell Science*, *82*, 223-234.
503 Lin, I. T., & Yao, M. C. (2020). Selfing mutants link Ku proteins to mating type determination in
504 *Tetrahymena*. *PLOS Biology*, *18*(8), e3000756. https://doi.org/10.1371/journal.pbio.3000756
505 Ma, Y., Yan, G., Han, X., Zhang, J., Xiong, J., & Miao, W. (2020). Sexual cell cycle initiation is regulated
506 by CDK19 and CYC9 in *Tetrahymena thermophila*. *Journal of Cell Science*, *133*(6).
507 https://doi.org/10.1242/jcs.235721
508 Mellacheruvu, D., Wright, Z., Couzens, A. L., Lambert, J. P., St-Denis, N. A., Li, T., Miteva, Y. V., Hauri, S.,
509 Sardiu, M. E., Low, T. Y., Halim, V. A., Bagshaw, R. D., Hubner, N. C., Al-Hakim, A., Bouchard,
510 A., Faubert, D., Fermin, D., Dunham, W. H., Goudreault, M., . . . Nesvizhskii, A. I. (2013). The
511 CRAPome: a contaminant repository for affinity purification-mass spectrometry data. *Nature*
512 *methods*, *10*(8), 730-736. https://doi.org/10.1038/nmeth.2557

513 Mochizuki, K. (2008). High efficiency transformation of *Tetrahymena* using a codon-optimized
514 neomycin resistance gene. *Gene*, *425*(1-2), 79-83.
515 https://doi.org/10.1016/j.gene.2008.08.007
516 Nanney, D. L. (1953). Nucleo-Cytoplasmic Interaction during Conjugation in *Tetrahymena*. *Biological*
517 *Bulletin*, *105*(1), 133-148. https://doi.org/10.2307/1538562
518 Orias, E. (1981). Probable somatic DNA rearrangements in mating type determination in *Tetrahymena*
519 *thermophila*: A review and a model. *Developmental Genetics*, *2*(2), 185-202.
520 https://doi.org/doi:10.1002/dvg.1020020205
521 Orias, E., Cervantes, M. D., & Hamilton, E. P. (2011). *Tetrahymena thermophila*, a unicellular
522 eukaryote with separate germline and somatic genomes. *Research in Microbiology*, *162*(6),
523 578-586. https://doi.org/10.1016/j.resmic.2011.05.001
524 Orias, E., Singh, D. P., & Meyer, E. (2017). Genetics and Epigenetics of Mating Type Determination in
525 *Paramecium* and *Tetrahymena*. *Annual Review of Microbiology*, *71*(1).
526 Phadke, S. S., & Zufall, R. A. (2010). Rapid diversification of mating systems in ciliates. *Biological*
527 *Journal of the Linnean Society*, *98*(1), 187-197.
528 Sieber, B., Coronas-Serna, J. M., & Martin, S. G. (2023). A focus on yeast mating: From pheromone
529 signaling to cell-cell fusion. *Seminars in Cell & Developmental Biology*, *133*, 83-95.
530 https://doi.org/10.1016/j.semcdb.2022.02.003
531 Singh, D. P., Saudemont, B., Guglielmi, G., Arnaiz, O., Gout, J. F., Prajer, M., Potekhin, A., Przybos, E.,
532 Aubusson-Fleury, A., Bhullar, S., Bouhouche, K., Lhuillier-Akakpo, M., Tanty, V., Blugeon, C.,
533 Alberti, A., Labadie, K., Aury, J. M., Sperling, L., Duharcourt, S., & Meyer, E. (2014). Genome-
534 defence small RNAs exapted for epigenetic mating-type inheritance. *Nature*, *509*(7501), 447-
535 452. https://doi.org/10.1038/nature13318
536 Takayama, S., & Isogai, A. (2005). Self-incompatibility in plants. *Annual Review of Plant Biology*, *56*(1),
537 467-489. https://doi.org/10.1146/annurev.arplant.56.032604.144249
538 Tian, M., Yang, W., Zhang, J., Dang, H., Lu, X., Fu, C., & Miao, W. (2017). Nonsense-mediated mRNA
539 decay in *Tetrahymena* is EJC independent and requires a protozoa-specific nuclease. *Nucleic*
540 *Acids Research*, *45*(11), 6848-6863. https://doi.org/10.1093/nar/gkx256
541 Vekemans, X., & Castric, V. (2021). When the genetic architecture matters: evolutionary and
542 ecological implications of self versus nonself recognition in plant self‐incompatibility. *New*
543 *Phytologist*, *231*(4), 1304-1307. https://doi.org/10.1111/nph.17471
544 Wang, G., Chen, K., Zhang, J., Deng, S., Xiong, J., He, X., Fu, Y., & Miao, W. (2020). Drivers of Mating
545 Type Composition in *Tetrahymena thermophila*. *Genome Biology and Evolution*, *12*(12),
546 2328-2343. https://doi.org/10.1093/gbe/evaa197
547 Wang, S., Gao, D., Penny, J., Krishna, S., & Takeyasu, K. (1997). P-Type ATPases in *Tetrahymena*.
548 *Annals of the New York Academy of Sciences*, *834*(1), 158-160.
549 https://doi.org/10.1111/j.1749-6632.1997.tb52247.x
550 Wang, S., & Takeyasu, K. (1997). Primary structure and evolution of the ATP-binding domains of the P-
551 type ATPases in *Tetrahymena thermophila*. *American Journal of Physiology*, *272*(2 Pt 1),
552 C715-728. https://doi.org/10.1152/ajpcell.1997.272.2.C715

553 Wolfe, J., & Feng, S. (1988). Concanavalin A receptor 'tipping' in *Tetrahymena* and its relationship to
554 cell adhesion during conjugation. *Development*, *102*(4), 699.
555 http://dev.biologists.org/content/102/4/699.abstract
556 Wolfe, J., & Grimes, G. W. (1979). Tip Transformation in *Tetrahymena*: A Morphogenetic Response to
557 Interactions Between Mating Types. *The Journal of Protozoology*, *26*(1), 82-89.
558 https://doi.org/10.1111/j.1550-7408.1979.tb02737.x
559 Wolfe, J., Pagliaro, L., & Fortune, H. (1986). Coordination of concanavalin-A-receptor distribution and
560 surface differentiation in *Tetrahymena*. *Differentiation*, *31*(1), 1-9.
561 https://doi.org/https://doi.org/10.1111/j.1432-0436.1986.tb00375.x
562 Wu, J., Wang, S., Gu, Y., Zhang, S., Publicover, S. J., & Franklin-Tong, V. E. (2011). Self-incompatibility
563 in *Papaver rhoeas* activates nonspecific cation conductance permeable to Ca2+ and K+. *Plant*
564 *Physiology*, *155*(2), 963-973. https://doi.org/10.1104/pp.110.161927
565 Xiong, J., Lu, X., Lu, Y., Zeng, H., Yuan, D., Feng, L., Chang, Y., Bowen, J., Gorovsky, M., Fu, C., & Miao,
566 W. (2011). *Tetrahymena* Gene Expression Database (TGED): a resource of microarray data
567 and co-expression analyses for *Tetrahymena*. *Sci China Life Sci*, *54*(1), 65-67.
568 https://doi.org/10.1007/s11427-010-4114-1
569 Yan, G., Yang, W., Han, X., Chen, K., Xiong, J., Hamilton, E. P., Orias, E., & Miao, W. (2021). Evolution of
570 the mating type gene pair and multiple sexes in *Tetrahymena*. *iScience*, *24*(1), 101950.
571 https://doi.org/10.1016/j.isci.2020.101950
572 Zhou, Y., Fu, L., Mochizuki, K., Xiong, J., Miao, W., & Wang, G. (2022). Absolute quantification of
573 chromosome copy numbers in the polyploid macronucleus of *Tetrahymena thermophila* at
574 the single-cell level. *Journal of Eukaryotic Microbiology*, *69*(4), e12907.
575 https://doi.org/10.1111/jeu.12907
576

577 ## Figure legends

578 **Figure 1. Mating-type recognition in *T. thermophila*.** (**A**) Example of self and non-self mating-
579 type recognition. When one cell of mating type I encounters another, costimulation and mating
580 do not occur. When a cell of mating type I encounters a cell of another mating type (II–VII), the
581 cells enter the costimulation stage and go on to form a pair. (**B**) Two typical phenotypes of the
582 costimulation stage are Tip transformation and Con-A receptor appearance. Yellow dashed circle,
583 transformed cell tip (center, single cell) or pairing junction (right, cell pair). Note that Tip
584 transformation may become less obvious after Con-A staining. (**C**) *MTA* and *MTB* gene structure
585 and MTA and MTB protein domain information (Cervantes et al., 2013). MTA and MTB form a

586 head-to-head gene pair. For each gene, the terminal exon is shared by all mating types and the
587 remainder is mating-type-specific (the sequence differs for each mating type). The mating-type-
588 specific region of each protein is predicted to be extracellular.

589 **Figure 2. Mating-type proteins are essential for mating-type recognition.** (**A**) Experimental
590 procedure for the costimulation experiments. Starved WT cells of mating types V (WT-V) and VII
591 (WT-VII) were separately pre-incubated with the indicated mating type VI mutant (9 : 1 ratio) for
592 30 min and then the pre-incubated cells were mixed at a 1 : 1 ratio. Note that before mixing the
593 costimulated cells, any potentially pairing cells were separated by shaking. (**B**) Effect of pre-
594 incubation with Δ*MTA* and Δ*MTB* on the rate of pair formation. Each experiment was repeated
595 three times, with > 100 pairs counted at each time point. Matched two-way ANOVA was used for
596 the statistical analysis. N.S., not significant; *, $P < 0.05$; **, $P < 0.01$; ***, $P < 0.001$; ****,
597 $P < 0.0001$. Unpaired mutants were excluded when calculating the pairing rate (see Materials
598 and Methods). (**C**) Tip transformation, a hallmark of costimulation. Each strain was pre-incubated
599 with the strain shown in subscript. Yellow dashed circle, transformed cell tip. (**D**) Appearance of
600 Con-A receptors, another hallmark of costimulation. In all, ~90% cells show Con-A receptor
601 fluorescence (panels 4, 5 and 9). The low percentage of cells (7%) with fluorescence in panel 7
602 were probably WT cells, which comprised 10% of the pre-incubation culture. Each strain was pre-
603 incubated with the strain shown in subscript. Yellow dashed circle, Con-A receptor fluorescence.

604 **Figure 3. Proteins that interact with MTA and MTB.** (**A**) Construction of HA-tagged strains. All of
605 the tagged strains mated like WT cells. (**B**) Statistical analysis of IP-MS data. A total of 13
606 experiments were carried out. WT samples (untagged) were run in parallel for each sample. All

607 13 WT controls were combined as the background control. Red dot, high-confidence interaction;
608 dark gray dot, low-confidence interaction. Gene identifiers are summarized in Figure 3–Source
609 data 2. Note that the wash buffer contained 1% Triton X-100 and 600 mM NaCl. (**C**) Interaction
610 network based on IP-MS data. Orange oval, bait; blue oval, high-confidence prey; light gray dot,
611 low-confidence prey; black line, high-confidence interaction; dark gray dashed line, low-
612 confidence interaction; light gray dotted line, interaction supported by a few peptides (these
613 proteins were shown because their coding genes are coexpressed with *MTA* and *MTB* and
614 deleting them affects mating behavior). (**D**) Diagram of functional domain annotation of MTRC
615 components. GFR, growth factor receptor domain; PLF, pectin lyase fold; Poly-E, poly-glutamic
616 acid region; NTH, P-loop-containing nucleotide triphosphate hydrolase. (**E**) Expression profiles of
617 genes whose protein products were identified by IP-MS as potentially components of the MTRC.
618 Expression data is derived from *Tetra*FGD (Xiong et al., 2011).

619 **Figure 4. Mating-type proteins are cell surface proteins but do not localize to cilia.** (**A**)
620 Fractionation of *MTA7-HA* cells (please see Figure 4–figure supplement 1A for the experimental
621 process). Red arrowhead, MTA7-HA; F, flow through; P, pellet; R, resin; S, supernatant; W, wash.
622 The MTA signal is undetectable until S3 (enriched membrane proteins), and only appears after
623 affinity chromatography (R). (**B**) WB analysis of cell surface proteins. Red arrowhead, MTA7-HA;
624 M, marker; C, negative control (unbiotinylated). (**C**) Cilia isolation and purification. (**D**) WB
625 analysis of IP products of membrane and ciliary proteins. Mem, membrane; R, resin; S,
626 supernatant. The same amount of *MTA7-HA* cells was used for the membrane and ciliary protein
627 IPs. The full blot is shown in Figure 4–figure supplement 1B. (**E**) Construction scheme for eGFP-

628 tagged MTB2 strains. (**F**) Costimulated *MTB2-eGFP* cell. (**G**) Paired *MTB2-eGFP* x WT cell. To
629 induce MTB2-eGFP overexpression, cells were treated with 10 ng/ml Cd^{2+} for 5 h. Green, eGFP
630 signal; red, tubulin signal; yellow dashed line, cell outline. The focal plane of these images is the
631 cell surface.

632 **Figure 5. Stimulation experiments using MTAxc and/or MTBxc.** (**A**) WT cells were treated with
633 MTAxc and/or MTBxc proteins (30 pg/ml, 1 h) of different mating-type specificities. WT-VI cells
634 were treated with MTA/B7xc protein, and WT-VII cells were treated with MTA/B6xc protein.
635 Treated cells were washed twice before mixing to remove residual proteins from the starvation
636 medium. Note that the starvation medium used for washing should contain mating-essential
637 factors secreted by *T. thermophila* cells during starvation (Adair et al., 1978). The mating types
638 used in each experiment is shown in the figure. Each strain was pre-incubated with the strain
639 shown in subscript. Each experiment was repeated five times. (**B, C**) The percentages of cells
640 paired at 60 min (**B**) and 75 min (**C**) were used for the statistical analysis (method described in
641 Figure 2B). (**D**) WT cells (mating types VI and VII) were treated with MTAxc and/or MTBxc
642 proteins of the same mating-type specificity (as described in (**A**)). (**E, F**) The percentages of cells
643 paired at 75 min (**E**) and 240 min (**F**) were used for the statistical analysis (method described in
644 Figure 2B).

645 **Figure 6. Results of treatment with either MTAxc or MTBxc proteins.** (**A**–**F**) Dose–response
646 effect of treatment with MTA6xc or MTB6xc protein. (**A**–**C**) MTA6xc results. (**D**–**F**) MTB6xc results.
647 Cells of mating types I and VII were used for these experiments. Experimental and statistical

648 methods were as described for Figure 5, except for protein concentrations. (**G**–**J**) MTA6xc or
649 MTB6xc proteins affect the mating of various combinations of other WT mating types. (**G**)
650 MTA6xc results. Both mating partners were treated. (**H**) MTB6xc results. Both mating partners
651 were treated. (**I**) MTA6xc results. Cells of only one mating type were treated. Note that mating
652 type VI cells were used in these experiments. (**J**) MTB6xc results. Note that mating type VI cells
653 were used in these experiments. Experimental and statistical methods were as described for
654 Figure 5. The mating types used in each experiment is shown in the figure. Red subscript "A6" or
655 "B6" in (**G-J**) indicate the strain treated with MTA6xc or MTB6xc, respectively.

656 **Figure 7. A hypothesized mating-type recognition model.** MTA and MTB function by forming
657 MTRC with several other proteins. When cells of the same mating type contact each other, the
658 interaction between MTRCs inhibits mating. Conversely, when cells of different mating types
659 contact each other, the interaction between MTRCs initiates mating. Many details remain
660 unknown, such as (i) during self-recognition, whether the MTRC is only blocked or generates an
661 inhibitory signal (e.g., membrane potential by Ca^{2+}), (ii) how two MTRCs interact during cell-cell
662 recognition, and the differences between self- and non-self-recognition, and (iii) the downstream
663 pathway when MTRC is activated. We hope future studies will help refine and advance this
664 model, contributing to a comprehensive understanding of how mating types are recognized in
665 multiple mating systems.

666 **Supplementary Information**

667 **Figure 1 – figure supplement 1. *T. thermophila* lifecycle.** *T. thermophila* has seven mating types.
668 Cells divide asexually when nutrition is adequate. After starvation, cells of any two different

669 mating types recognize each other and enter a pre-conjugation stage called costimulation. In this
670 stage, cells first become round (Fujishima et al., 1993); subsequently, their cell tips are
671 transformed into a curved shape (Wolfe & Grimes, 1979) and the Con-A receptor becomes
672 detectable (Wolfe & Feng, 1988; Wolfe et al., 1986). Costimulated cells then form pairs via a
673 rotating behavior (Video S1, S2). *T. thermophila* possesses two types of nuclei within a single cell:
674 the somatic macronucleus (MAC, ~90N) (Zhou et al., 2022) and the germline micronucleus (MIC,
675 2N). The *mat* locus on the MIC chromosome contains several mating-type gene pairs (mtGP,
676 including *MTA* and *MTB*) organized in a tandem array. In contrast, the MAC chromosome carries
677 only one mtGP. During the sexual life cycle (conjugation), cells undergo a series of sexual events.
678 MIC undergo meiosis and reciprocal fertilization (for details refer to (Orias et al., 2011)). The new
679 MAC of progeny develops from the fertilization MIC through a series of genome editing events,
680 and increase its ploidy to ~90 via endoreduplication. During this process, mtGP loss occurs,
681 resulting in only one mtGP remaining on the MAC chromosome. The mating-type specificity of
682 mtGPs on each chromosome within one nucleus becomes pure to some extant relatively quickly,
683 a phenomenon termed intranuclear coordination. Exconjugants (separated pairs) finally form
684 parent-like progeny when nutrition becomes available, but remain sexually immature. After
685 ~60 fissions, cells mature and their mating type is determined and becomes fixed (for details of
686 mating-type determination, the interested readers is referred to (Orias et al., 2017)).

687 **Figure 2 – figure supplement 1. Mating-type gene deletion strains do not costimulate WT cells.**
688 (**A**) Pre-incubation results predicted by a simple receptor–ligand model of mating-type
689 recognition, in which one mating-type protein is designed ligand (L) and the other receptor (R).

690 The type of cell used to costimulate is shown on the left. The expected result of costimulation if
691 *T. thermophila* were to use non-self mating-type recognition (1, 3, 5) or self mating-type
692 recognition (2, 4, 6). If this simple model were true, deleting the receptor would have a different
693 effect on costimulation to deleting the ligand. However, the experimental results showed that
694 neither Δ*MTA* nor Δ*MTB* can fully transmit/receive mating signal to/from WT cells. Therefore,
695 mating-type recognition in *T. thermophila* does not occur via the simple receptor–ligand binding
696 mechanism. Costim, costimulation. (**B**) Construction method of gene deletion strains. (**C**) Pre-
697 incubation with Δ*MTA* or Δ*MTB* does not influence the pairing rate. The experimental method
698 was as described in Figure 2A except that the pre-incubation time was 16 h. (**D**-**G**) Diagram
699 illustrating a theoretical mating-type recognition model between WT cells and Δ*CDK19*, Δ*CYC9*
700 cells, MTAxc, MTBxc proteins and Δ*MTA*, Δ*MTB* cells. (**D**-**E**) In WT or Δ*CDK19*, Δ*CYC9* cells, where
701 MTA and MTB proteins are expressed on the same cells, they can combine and stimulate another
702 WT cells during attachment. (**F**) MTAxc and MTBxc proteins, being freely diffusible in solution,
703 can continuously stimulate the WT cell. Moreover, MTAxc and MTBxc proteins have the
704 opportunity to combine, providing a stronger stimulation. (**G**) In Δ*MTA* and Δ*MTB* cells, MTB and
705 MTA proteins integrated into the cytomembrane of different cells and so cannot combine and
706 stimulate the WT cells (i.e., WT cell receive one type of signal at a time, the signal stops when
707 two cells separate).

708 **Figure 4 – figure supplement 1. Cell fractionation MTA7-HA cells.** (**A**) Experimental process for
709 cell fractionation. (**B**) Affinity purification results of the soluble pool (S2, shown in panel A) and
710 ciliary protein. C+, positive control (i.e., IP product of MTA7-HA cell membrane); R, resin; S,

711 supernatant. No MTA7-HA signal was detected in the soluble pool or in ciliary protein samples,

712 even after affinity purification.

713 **Figure 4 – figure supplement 2. Confocal images of ciliary sections and cell interior sections of**

714 ***MTB2-eGFP* cells.** (**A**) No MTB2-eGFP signal was associated with cilia. (**B**) In the cell interior

715 section, MTB2-eGFP protein was detected on the plasma membrane and in intracellular

716 structures, probably the ER and Golgi.

717 **Figure 5 – figure supplement 1. Expression and purification of extracellular regions of mating-**

718 **type proteins.** (**A**) Schematic diagram showing truncated and full-sized proteins. (**B**–**E**) Size-

719 exclusion chromatography for MTA6xc (**B**), MTB6xc (**C**), MTA7xc (**D**), and MTB7xc (**E**). Left,

720 elution profile; right, Coomassie blue staining. In, input; M, marker.

721 **Figure 5 – figure supplement 2. Treatment with MTA6xc and/or MTB6xc proteins fails to**

722 **induce costimulation.** (**A**) Tip transformation. Yellow dashed circle, transformed cell tip. (**B**) Con-

723 A receptor appearance. Yellow dashed circle, Con-A signal. Cells of mating type VII were used for

724 these experiments.

725 **Video 1. Mating behavior of *T. thermophila*.**

726 **Video 2. Mating behavior of *T. thermophila*.** To distinguish cells of different mating types,

727 smaller mating type VI cells and larger mating type VII cells were used in this experiment.

728 **Video 3. Cells of different mating types form a pair, whereas cells of the same mating type**

729 **become separated after a short contact.** To distinguish cells of different mating types, smaller

730 mating type VI cells and larger mating type VII cells were used in this experiment.

731 **Figure 3–Source data 1. IP-MS results.**

732 **Figure 3–Source data 2. Gene identifiers.**

733 **Figure 4–Source data 1. MS analysis of MTA7-HA cilia protein.**

734 **Figure 4–Source data 2. MS analysis of *MTB2-eGFP* cilia protein.**

735 **Appendix 1—table 1. Strains used in this study.**

736 **Appendix 1—table 2. Primers used in this study.**

Figure 1

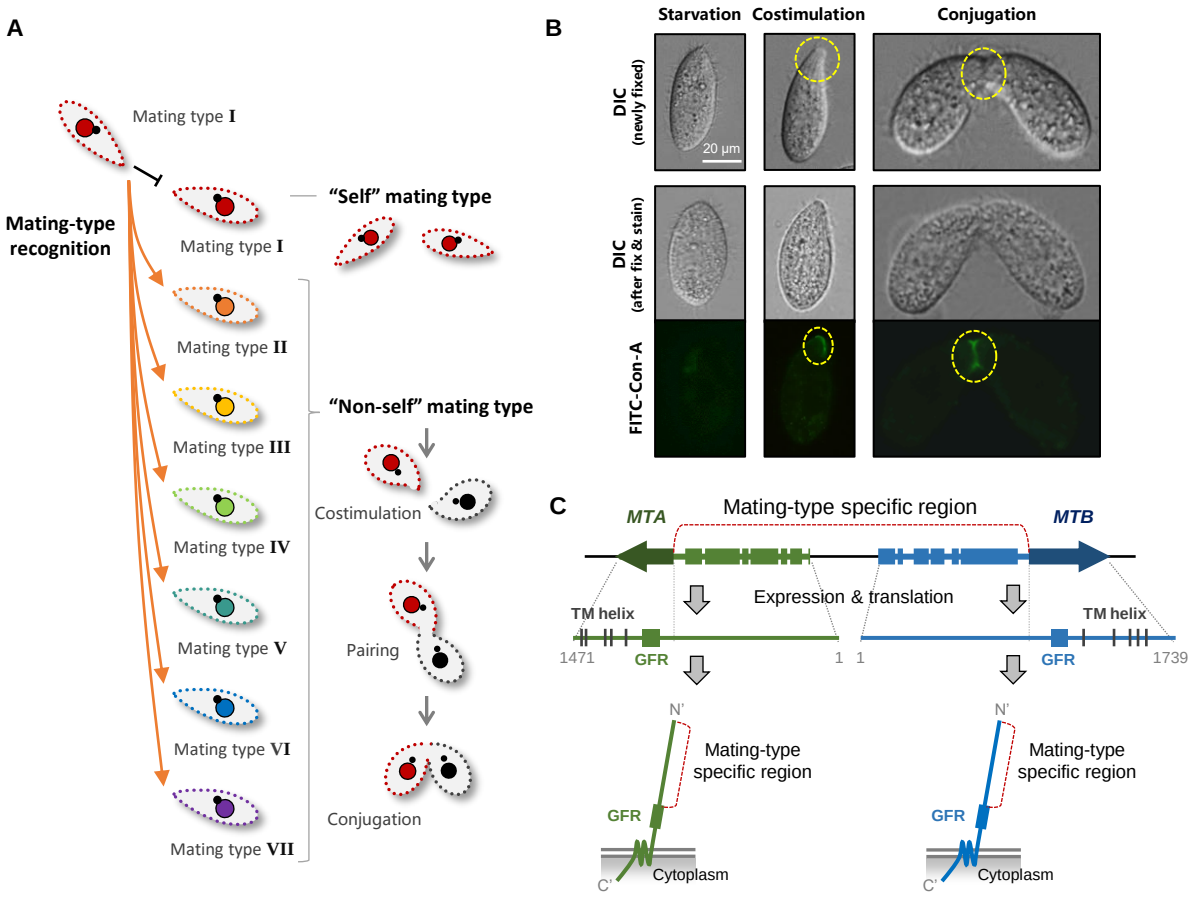
A
Mating type I
Mating-type recognition
Mating type I
"Self" mating type
Mating type II
Mating type III
"Non-self" mating type
Mating type IV
Costimulation
Mating type V
Pairing
Mating type VI
Conjugation
Mating type VII
B
Starvation
Costimulation
Conjugation
DIC (newly fixed)
20 µm
DIC (after fix & stain)
FITC-Con-A
C
MTA
Mating-type specific region
MTB
Expression & translation
TM helix
TM helix
1471
GFR
1
1
GFR
1739
N'
Mating-type specific region
GFR
Cytoplasm
C'
N'
Mating-type specific region
GFR
Cytoplasm
C'

Figure 2

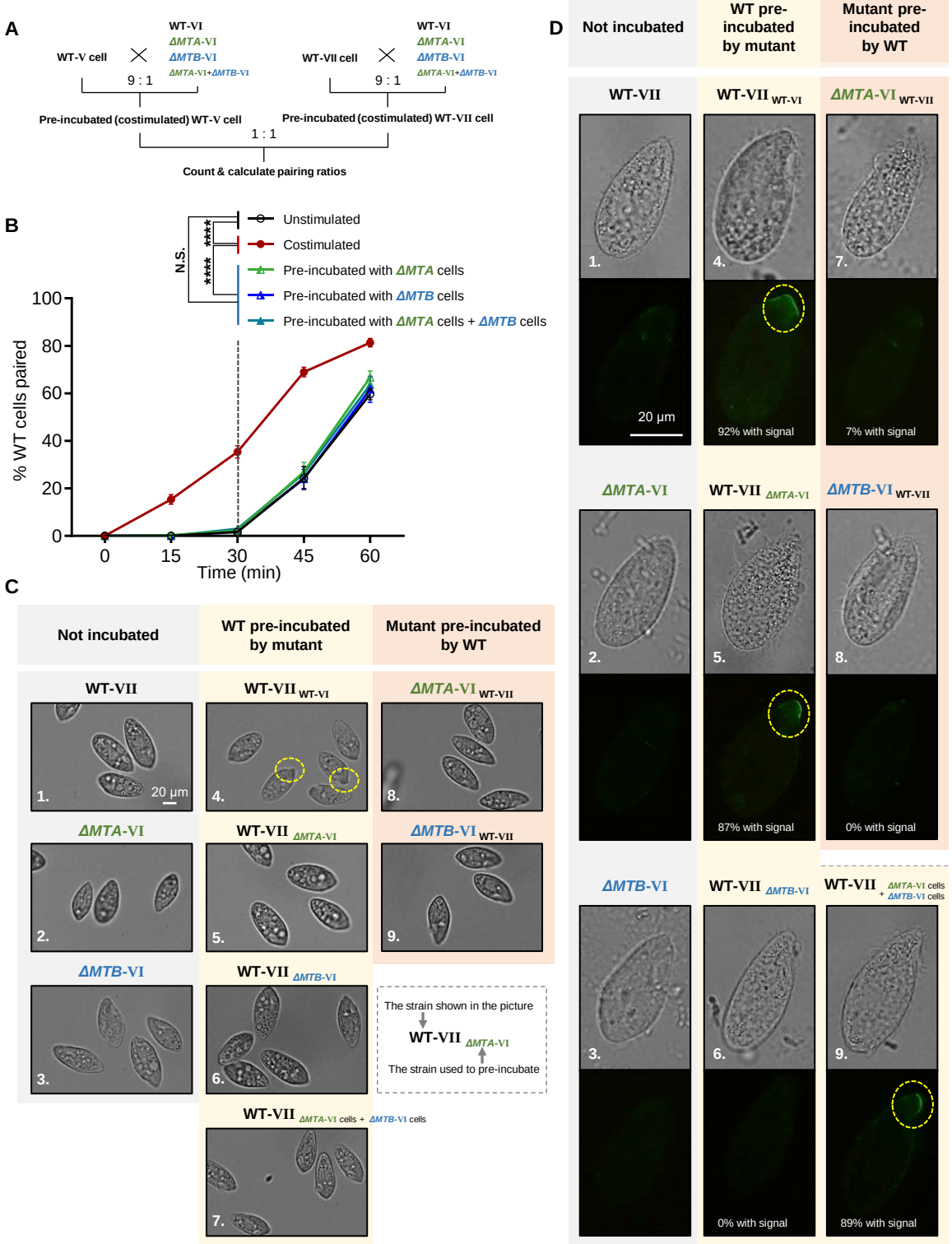
A
WT-V cell
WT-VI
ΔMTA-VI
ΔMTB-VI
ΔMTA-VI+ΔMTB-VI
9 : 1
WT-VII cell
WT-VI
ΔMTA-VI
ΔMTB-VI
ΔMTA-VI+ΔMTB-VI
9 : 1
Pre-incubated (costimulated) WT-V cell
Pre-incubated (costimulated) WT-VII cell
1 : 1
Count & calculate pairing ratios
B
Unstimulated
Costimulated
Pre-incubated with ΔMTA cells
Pre-incubated with ΔMTB cells
Pre-incubated with ΔMTA cells + ΔMTB cells
N.S.
****
****
% WT cells paired
100
80
60
40
20
0
0
15
30
45
60
Time (min)
C
Not incubated
WT pre-incubated by mutant
Mutant pre-incubated by WT
WT-VII
WT-VII WT-VI
ΔMTA-VI WT-VII
1.
20 µm
4.
8.
ΔMTA-VI
WT-VII ΔMTA-VI
ΔMTB-VI WT-VII
2.
5.
9.
ΔMTB-VI
WT-VII ΔMTB-VI
3.
6.
The strain shown in the picture
WT-VII ΔMTA-VI
The strain used to pre-incubate
WT-VII ΔMTA-VI cells + ΔMTB-VI cells
7.
D
Not incubated
WT pre-incubated by mutant
Mutant pre-incubated by WT
WT-VII
WT-VII WT-VI
ΔMTA-VI WT-VII
1.
4.
7.
20 µm
92% with signal
7% with signal
ΔMTA-VI
WT-VII ΔMTA-VI
ΔMTB-VI WT-VII
2.
5.
8.
87% with signal
0% with signal
ΔMTB-VI
WT-VII ΔMTB-VI
WT-VII ΔMTA-VI cells + ΔMTB-VI cells
3.
6.
9.
0% with signal
89% with signal

Figure 3

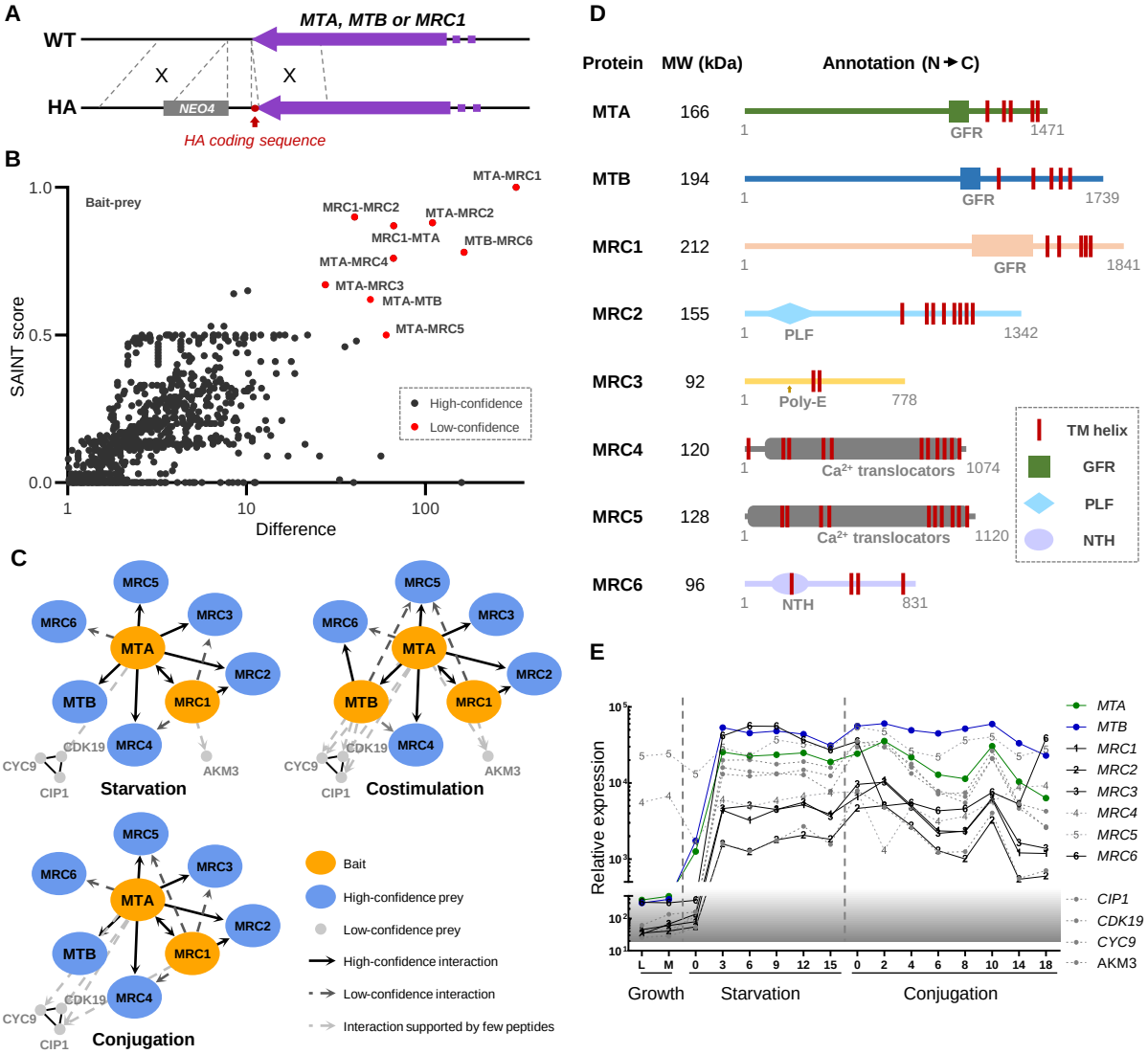
A
WT
MTA, MTB or MRC1
X
X
HA
NEO4
HA coding sequence
B
Bait-prey
SAINT score
Difference
1.0
0.5
0.0
1
10
100
MTA-MRC1
MRC1-MRC2
MTA-MRC2
MRC1-MTA
MTB-MRC6
MTA-MRC4
MTA-MRC3
MTA-MTB
MTA-MRC5
High-confidence
Low-confidence
C
MRC5
MRC6
MRC3
MTA
MRC2
MTB
MRC1
MRC4
CDK19
CYC9
CIP1
AKM3
Starvation
Costimulation
Conjugation
Bait
High-confidence prey
Low-confidence prey
High-confidence interaction
Low-confidence interaction
Interaction supported by few peptides
D
Protein
MW (kDa)
Annotation (N→C)
MTA 166 GFR 1471
MTB 194 GFR 1739
MRC1 212 GFR 1841
MRC2 155 PLF 1342
MRC3 92 Poly-E 778
MRC4 120 Ca2+ translocators 1074
MRC5 128 Ca2+ translocators 1120
MRC6 96 NTH 831
TM helix
GFR
PLF
NTH
E
Relative expression
MTA
MTB
MRC1
MRC2
MRC3
MRC4
MRC5
MRC6
CIP1
CDK19
CYC9
AKM3
L M 0 3 6 9 12 15 0 2 4 6 8 10 14 18
Growth
Starvation
Conjugation

Figure 4

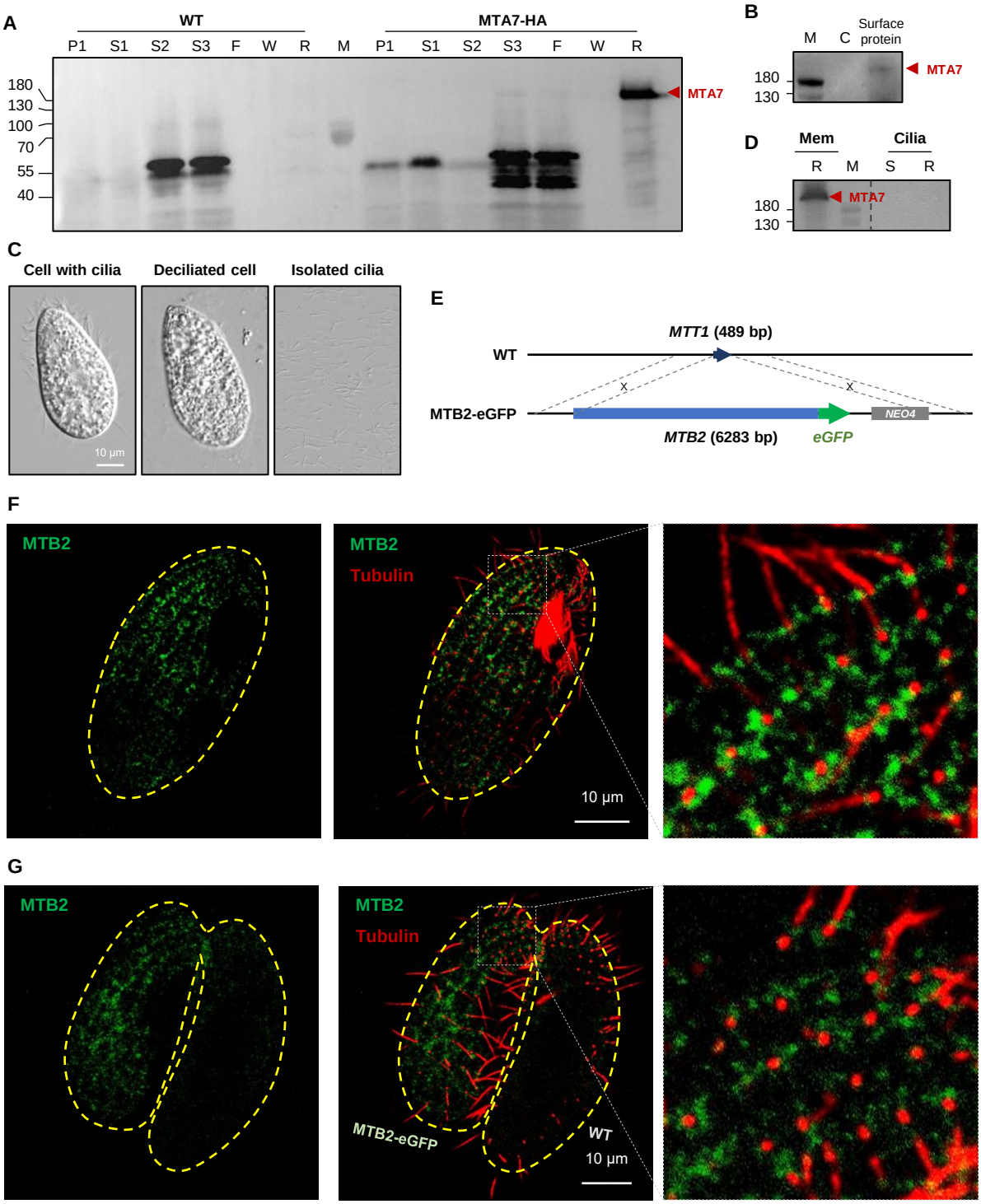
A
WT
MTA7-HA
P1 S1 S2 S3 F W R M P1 S1 S2 S3 F W R
180
130
100
70
55
40
MTA7
B
M C Surface protein
180
130
MTA7
D
Mem
Cilia
R M S R
180
130
MTA7
C
Cell with cilia
Deciliated cell
Isolated cilia
10 µm
E
MTT1 (489 bp)
WT
MTB2-eGFP
NEO4
MTB2 (6283 bp)
eGFP
F
MTB2
MTB2
Tubulin
10 µm
G
MTB2
MTB2
Tubulin
MTB2-eGFP
WT
10 µm

Figure 5

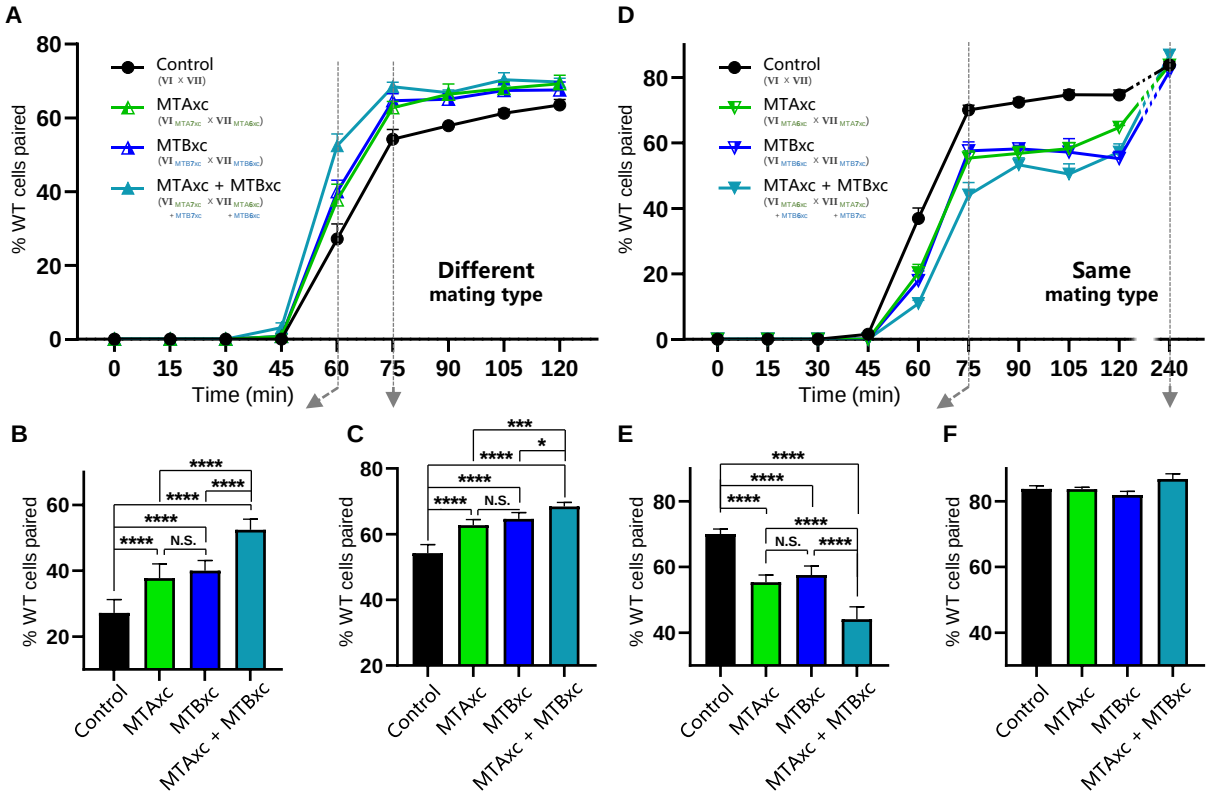
A
% WT cells paired
Control
(VI × VII)
MTAxc
(VI MTA7xc × VII MTA6xc)
MTBxc
(VI MTB7xc × VII MTB6xc)
MTAxc + MTBxc
(VI MTA7xc + MTB7xc × VII MTA6xc + MTB6xc)
Different
mating type
Time (min)
D
Same
mating type
B
C
E
F
N.S.
Control
MTAxc
MTBxc
MTAxc + MTBxc

Figure 6

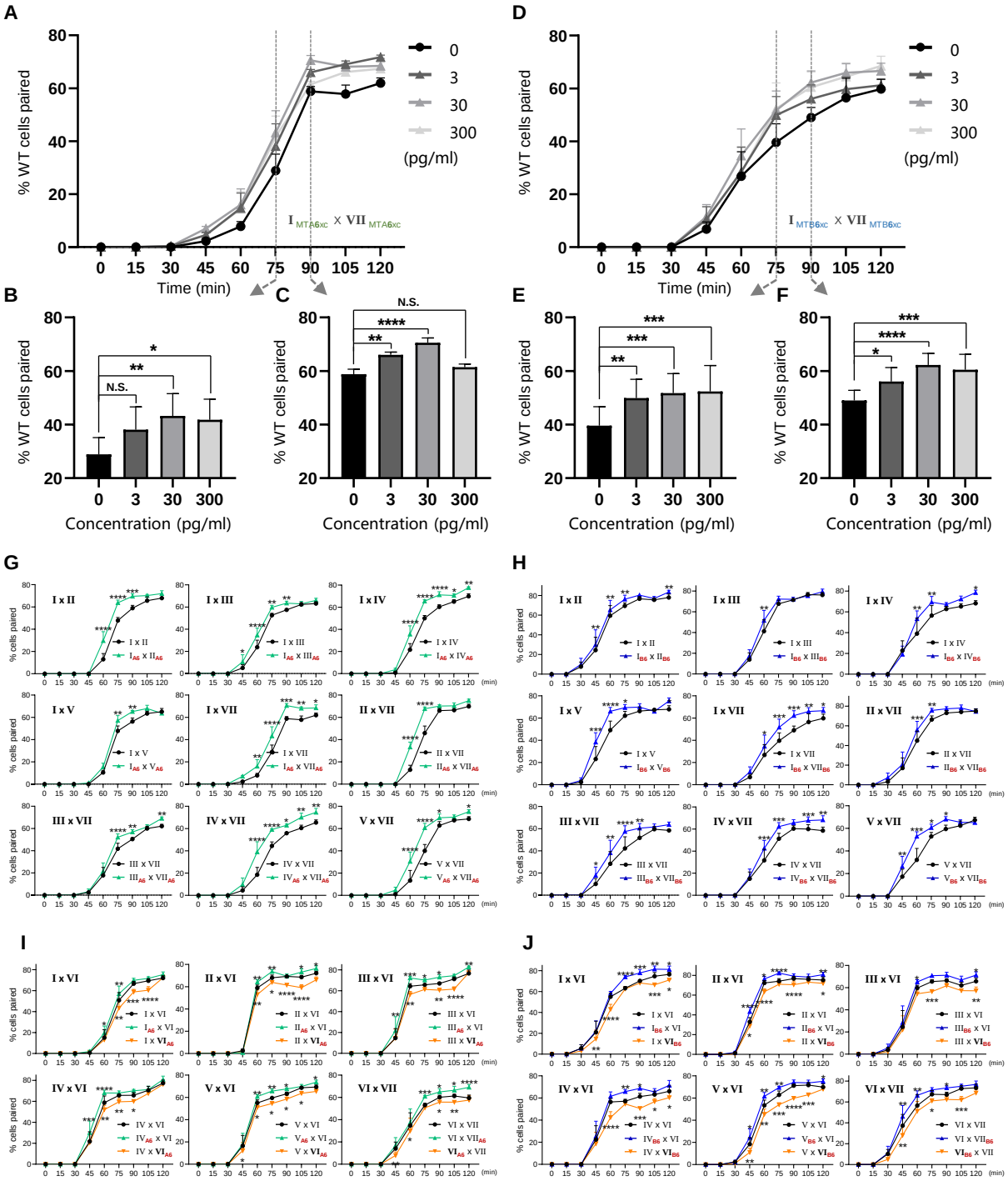
A
% WT cells paired
Time (min)
0
3
30
300
(pg/ml)
I MTA6xc X VII MTA6xc
D
I MTB6xc X VII MTB6xc
B
C
E
F
N.S.
Concentration (pg/ml)
G
H
I
J
% cells paired
(min)

Figure 7

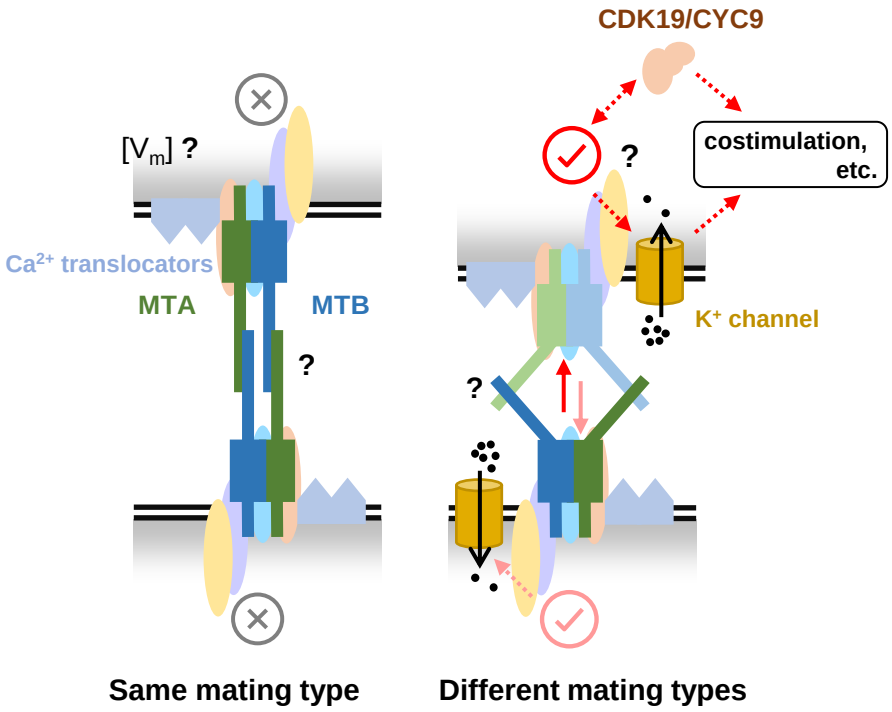
CDK19/CYC9
[Vm] ?
Ca2+ translocators
MTA
MTB
?
?
?
costimulation, etc.
K+ channel
Same mating type
Different mating types

Figure 1 – figure supplement 1

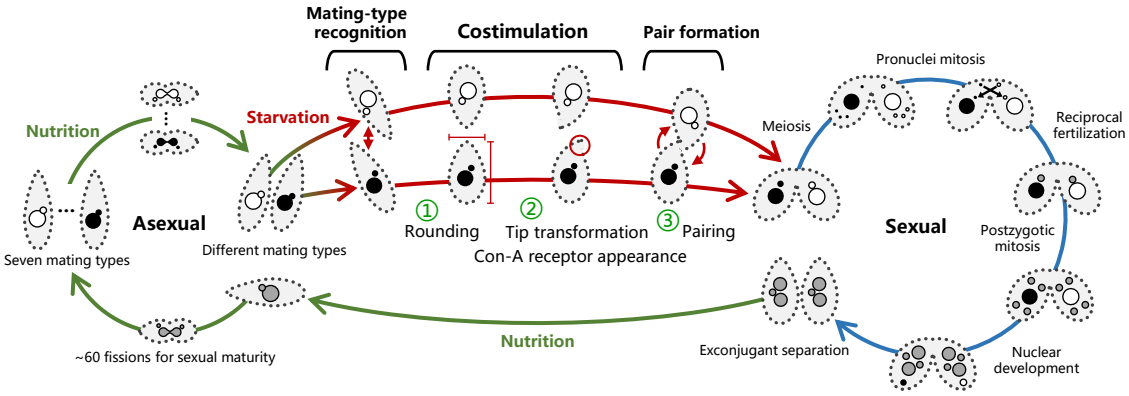

Figure 2 – figure supplement 1

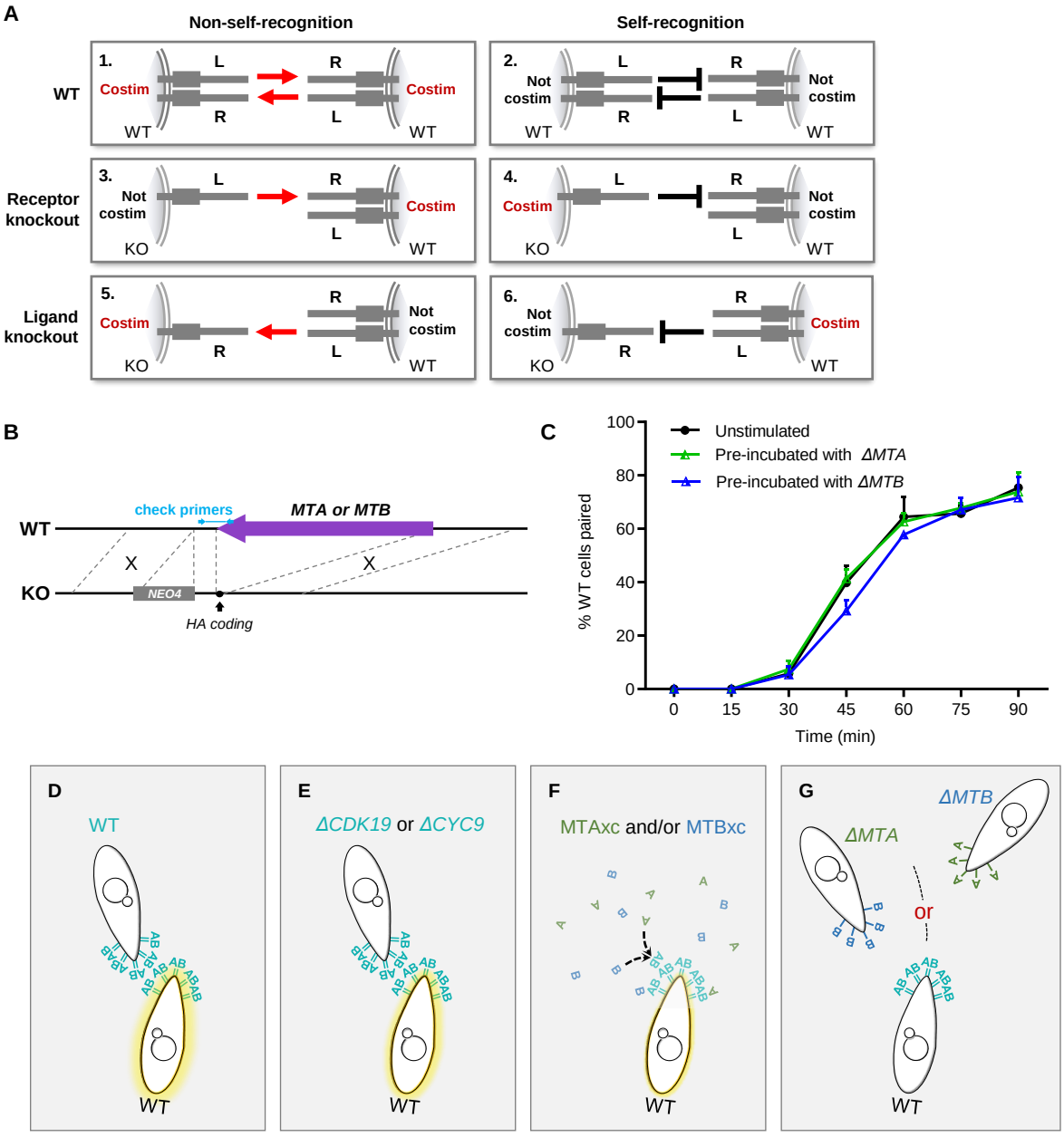

Figure 4 – figure supplement 1

A

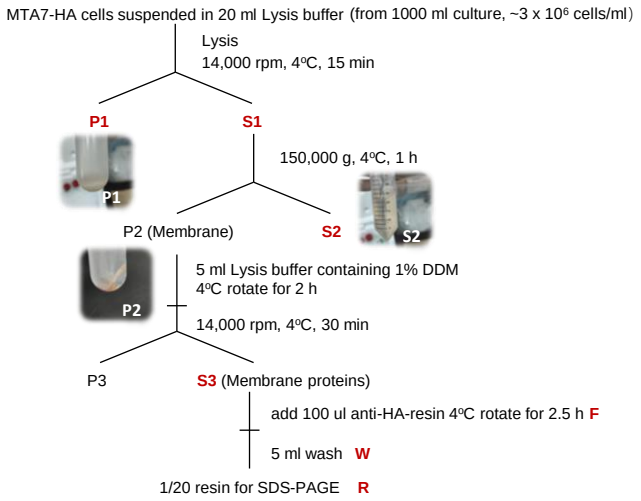

B

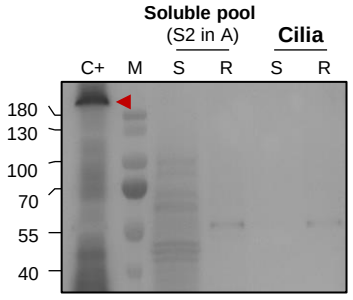

Figure 4 – figure supplement 2

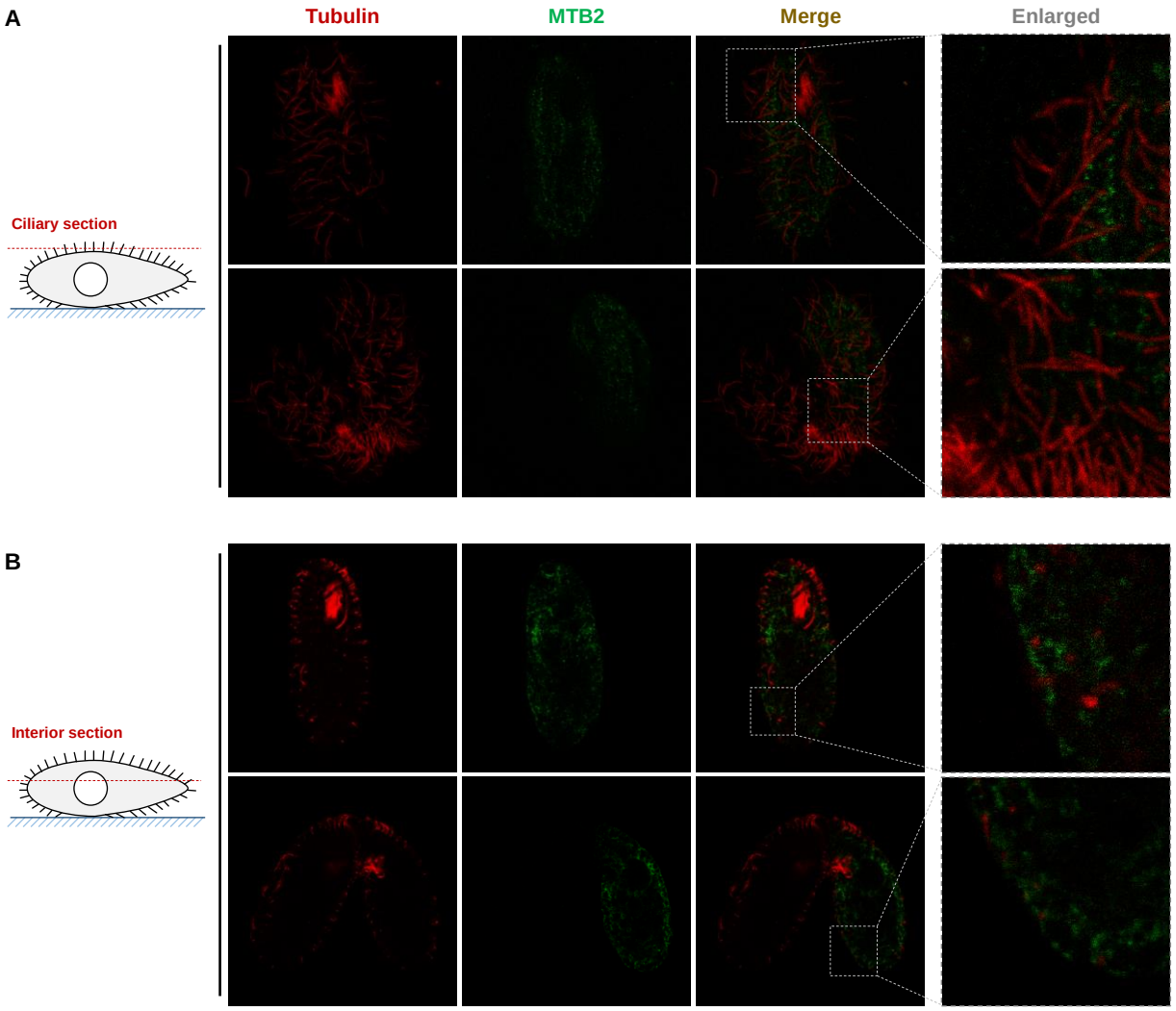

Figure 5 – figure supplement 1

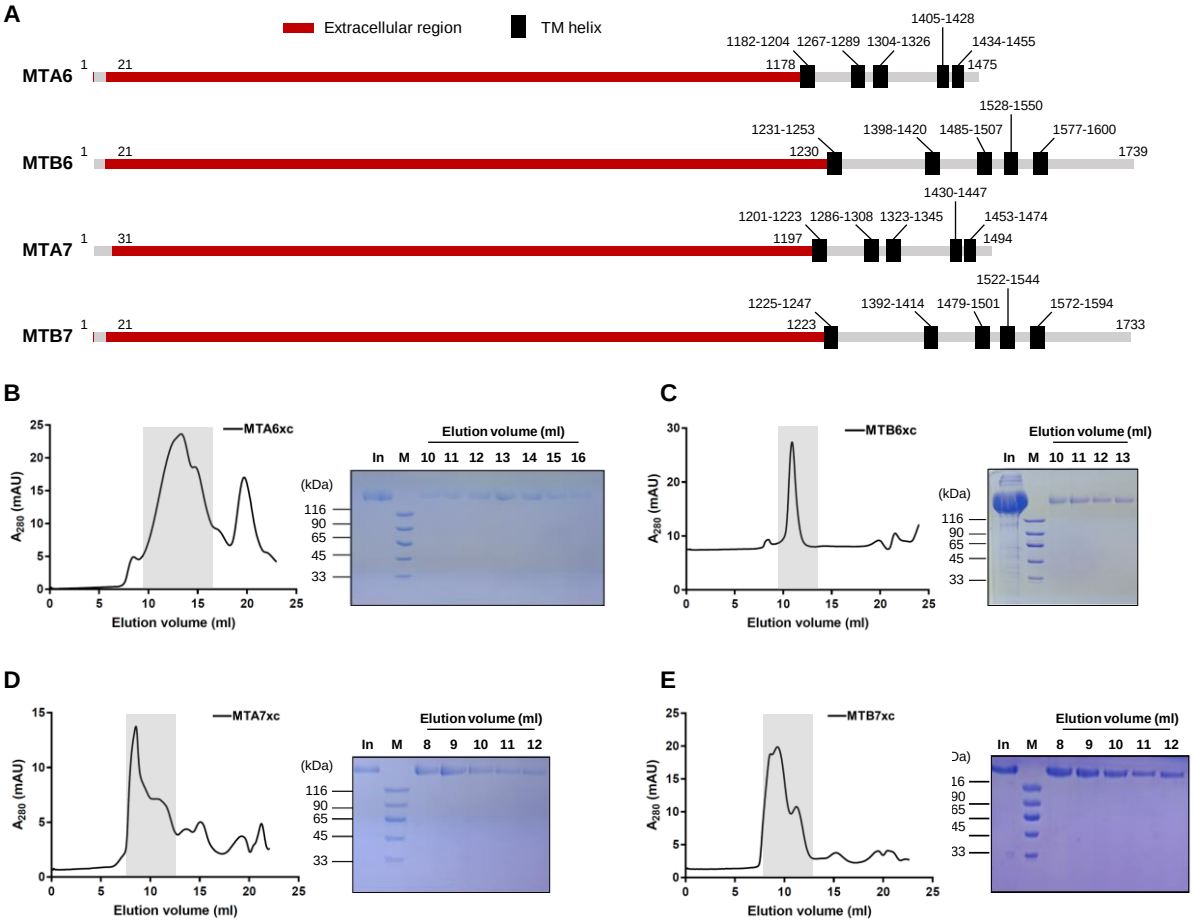
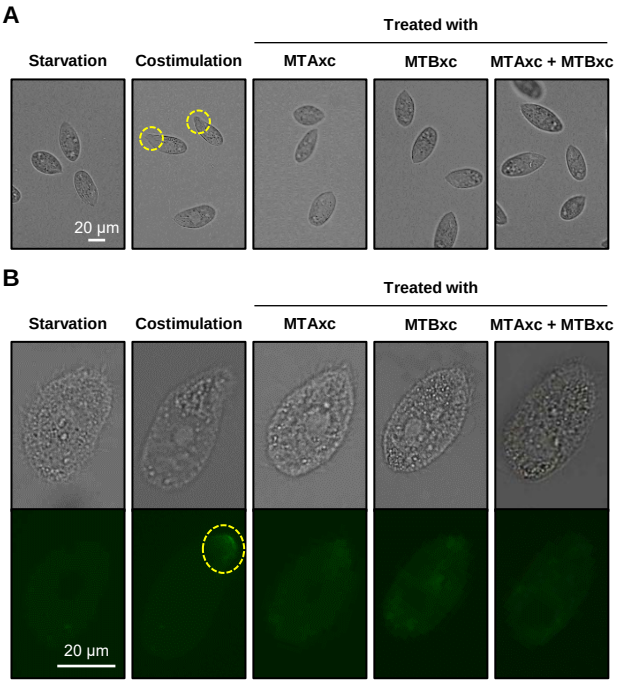
Figure 5 – figure supplement 2